JOC The Journal of Organic Chemistry

Article

pubs.acs.org/joc

Preparation of a Cyclic Polyphenylene Array for a Zigzag-Type Carbon Nanotube Segment

Ryuta Sekiguchi,[†] Kei Takahashi,[†] Jun Kawakami,[†] Atsushi Sakai,[‡] Hiroshi Ikeda,[‡,§] Aya Ishikawa,[∥] Kazuchika Ohta,[∥] and Shunji Ito*[,†]

[†]Graduate School of Science and Technology, Hirosaki University, Hirosaki 036-8561, Japan

[‡]Department of Applied Chemistry, Graduate School of Engineering, [§]The Research Institute for Molecular Electronic Devices (RIMED), Osaka Prefecture University, Osaka 599-8531, Japan

[∥]Smart Material Science and Technology, Interdisciplinary Graduate School of Science and Technology, Shinshu University, Ueda 386-8567, Japan

Supporting Information

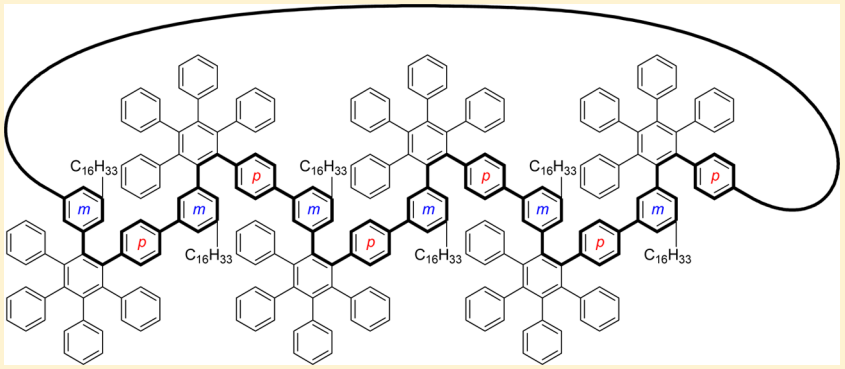

ABSTRACT: Preparation of cyclic polyphenylene array **2**, which corresponds to a complete carbon array of a zigzag-type CNT segment with (18,0)-structure, has been established by a Diels–Alder reaction of cyclic biphenylylene–acetylene derivative **1** with tetraphenylcyclopentadienone. The reaction of **2** with excess $FeCl_3$ realized a presumed cyclodehydrogenation reaction and elimination of the alkyl chains that were introduced as a measure to counter the low solubility problem, but this resulted in the formation of a complicated mixture that included the mass region of a presumed zigzag-type CNT segment with (18,0)-structure. The rather efficient blue emission of cyclic compounds **1** and **2** was discussed utilizing fluorescence (FL) quantum efficiencies (Φ_{FL}) and lifetimes (τ_{FL}) in their crystalline state along with those in dichloromethane solution. Thermal analyses of these compounds revealed their characteristic phase transition behavior. The synthesis of a novel cyclic polyphenylene array by utilizing a Diels–Alder reaction of cyclic phenylene–acetylene compounds with tetraphenylcyclopentadienone should afford an attractive pathway to a novel belt-shaped CNT segment.

INTRODUCTION

The bottom-up synthesis of hoop-shaped aromatic hydrocarbons is currently attracting interest because of their potential for use as a promising model of single-walled carbon nanotubes (CNTs). The representative synthesis of model compounds of this type is exemplified by the successful preparation of various [*n*]cycloparaphenylenes ([*n*]CPPs)[1] having a variety of ring sizes as the shortest models for armchair-type CNTs, which were produced by Jasti,[2] Itami,[3] and Yamago[4] over a several year period. Recent research interests have been shifted to the preparation of their congeners, such as [13]-cycloparaphenylene-2,6-naphtylene ([13]CPPN)[5] with a 2,6-naphtylene unit in the CPP nanohoop, for a model of a chiral-type CNT segment. The elongation of the hoop's width has also been examined by incorporating various kinds of polycyclicaromatic hydrocarbons into it, such as 1,4-naphthylene,[6] 2,7-pyrenylene,[7] 2,8-anthanthrylene,[8] 2,8-crysenylene,[9] 3,9-crysenylene,[10] a hexaphenylbenzene unit (as a promising precursor for hexa-*peri*-hexabenzocoronene (HBC)),[11] and so forth. Double-decker [*n*]CPPs[12] are another example of attempts to elongate the width of the hoop.

However, all examples of CPP congeners reported previously were constructed with a hoop of aromatic hydrocarbons, including fused-ring structures with single-bond linkages. Bottom-up synthesis of belt-shaped, cyclic π-electron systems that are totally composed of conjugated six-membered rings with fused-ring structures, such as cyclacenes, have still attracted attention, although the cyclacenes and their derivatives have not yet been synthesized.[13] To the best of our knowledge, the only successful examples of this kind of cyclic π-conjugated system are cyclophenacene congeners

Received: March 3, 2015
Published: April 21, 2015

DOI: 10.1021/acs.joc.5b00485
J. Org. Chem. 2015, 80, 5092–5110

constructed through top-down chemical synthesis from [60]-fullerene reported by Nakamura et al.[14]

More recently, an idea for the preparation of a polyphenylene array for the belt-shaped, cyclic π-electron system via cyclic phenylene–acetylene derivatives was proposed by Hughes et al.[15] However, there are no reports of the successful bottom-up synthesis of a cyclic polyphenylene array for belt-shaped π-electron systems via cyclic phenylene–acetylene derivatives.

Herein, we report the first synthesis of a cyclic polyphenylene array for a zigzag-type CNT segment with (18,0)-structure represented by using conventional assignments of the CNT's chiral indices.[1a,16] Notably, the present synthesis is the first example of the bottom-up construction of a large-sized cyclic polyphenylene array to produce a belt-shaped zigzag-type CNT segment via a Diels–Alder reaction of a cyclic biphenylylene–acetylene compound with tetraphenylcyclopentadienone. Transformation of the cyclic polyphenylene array to the zigzag-type CNT segment with (18,0)-structure was also examined. Efficient blue emission of the cyclic compounds in their solution and solid states was characterized by photophysical measurements, and the phase transition behavior of this new class of compounds was clarified by thermal analyses.

RESULTS AND DISCUSSION

Structural Principle. An efficient method for the preparation of HBC derivatives has been developed by Müllen et al.[17] We have applied this synthetic procedure to the preparation of a cyclic polyphenylene array to produce a zigzag-type CNT segment (Scheme 1).

Scheme 1. Synthetic Procedure for HBCs Developed by Müllen et al.[17]

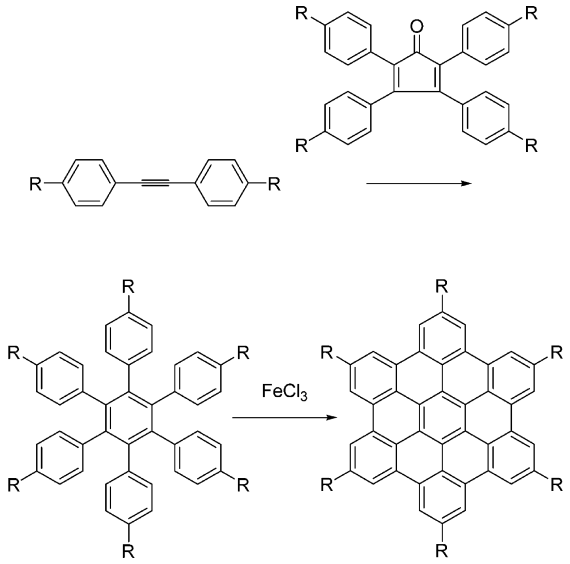

The idea for this comes from the arrangement of hexaphenylbenzene units on a graphene sheet. Once the terminal groups of the properly arranged hexaphenylbenzene units are connected with each other, the polyphenylene array should become a cyclic structure that corresponds to a proper polyphenylene array, yielding a CNT segment. The required cyclic phenylene–acetylene derivatives for the Diels–Alder reaction with tetraphenylcyclopentadienone that affords a presumed cyclic polyphenylene array could be designed on their own.

If the hexaphenylbenzene units are arranged as illustrated in Figure 1, then, for the preparation required, the cyclic

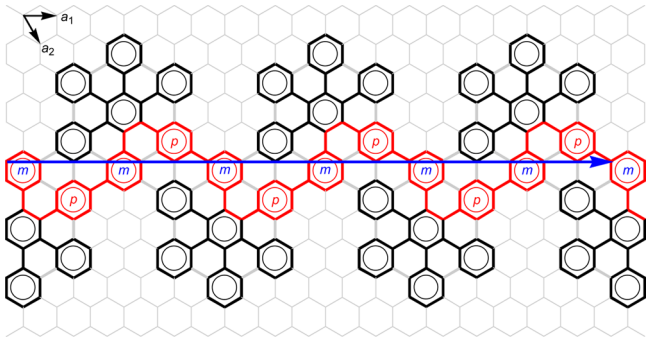

Figure 1. Structural principle: an array of hexaphenylbenzene units on a graphene sheet is used for the design of a zigzag-type CNT segment with (18,0)-structure. The short arrows, a_1 and a_2, represent two unit vectors that define the positions for rolling up the graphene sheet. The (18,0)-structure means that the graphene sheet is rolled up at the beginning of the blue arrow to the position that is 18 units along the a_1 vector and 0 units along the a_2 vector.

phenylene–acetylene derivative could be a cyclic structure, **1**, with a *meta*-phenylene–*para*-phenylene–acetylene–*meta*-phenylene–*para*-phenylene–acetylene linkage (Figure 2). For the

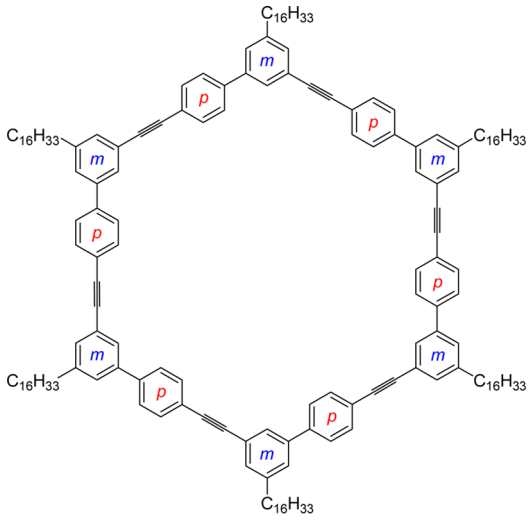

1

Figure 2. Cyclic biphenylylene–acetylene derivative **1** to produce a zigzag-type CNT segment with (18,0)-structure.

preparation of the cyclic biphenylylene–acetylene derivative **1**, we introduced a long alkyl chain in each biphenyl unit to prevent the low solubility of this kind of molecule. Macrocycle **1** was used to realize cyclic polyphenylene array **2**, which corresponds to a complete carbon array of a zigzag-type CNT segment with (18,0)-structure generated by a Diels–Alder reaction with tetraphenylcyclopentadienone (Figures 3 and 4).

In this strategy, cyclic polyphenylene array **2** could be prepared without serious steric hindrance during the synthetic scheme. Although the alkyl chains in **2** occupied positions that require a cyclodehydrogenation reaction, they should exhibit elimination by a *retro*-Friedel–Crafts reaction or migration to other positions under highly Lewis acidic cyclodehydrogenation conditions. The presumed tubular structure illustrated in Figure

DOI: 10.1021/acs.joc.5b00485
J. Org. Chem. 2015, 80, 5092–5110

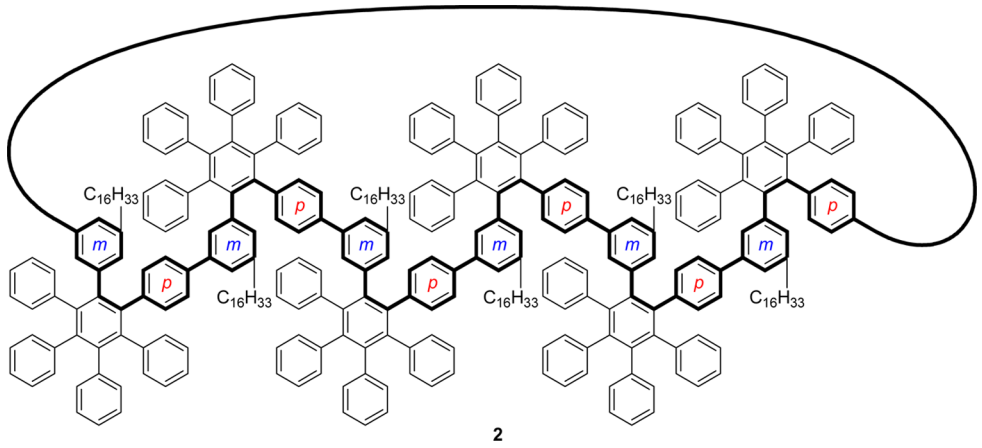

Figure 3. Cyclic polyphenylene array **2** to produce a zigzag-type CNT segment with (18,0)-structure.

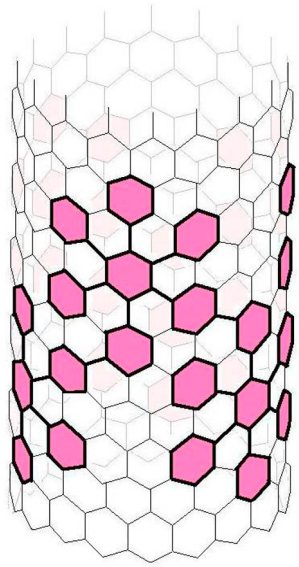

Figure 4. Representation of cyclic polyphenylene array **2** without the long alkyl chains in the zigzag-type CNT segment with (18,0)-structure.

5 should be thermodynamically stable because a CNT structure can be established by a physical procedure, such as by chemical vapor desorption. Thus, we expect the tubular structure to be formed at the final stage by a cyclodehydrogenation reaction. Unavoidable isomer problems during the cyclodehydrogenation step of **2** are discussed in the Cyclodehydrogenation Reaction section.

The present strategy for the Diels–Alder reaction of the cyclic biphenylylene–acetylene derivative with tetraphenylcyclopentadienone could be applied to produce a complete carbon array for a certain cylinder-like CNT segment with (6*n*,0)-structures by changing the ring size of the cyclic biphenylylene–acetylene derivatives. In addition, the arrangement of the hexaphenylbenzene units on the graphene sheet and the number of the units could properly be selected. Thus, the present approach may become a general procedure for producing a cyclic polyphenylene array with a variety of ring sizes and types to give a cylinder-like CNT segment by utilizing hexaphenylbenzene units as a LEGO block.

Synthesis. We synthesized cyclic polyphenylene array **2** through a Diels–Alder reaction of the corresponding cyclic biphenylylene–acetylene derivative **1** with tetraphenylcyclopentadienone (**3**); the strategy consisted of applying the synthesis of HBC derivatives. For the preparation of **1**, we utilized the repeated Sonogashira coupling reaction of iodide **4** and 3,3-diethyltriazene **5** as promising building blocks to synthesize the macrocycle (Figure 6).

Preparation of building blocks **4** and **5** commenced with 1,3,5-tribromobenzene (**6**) as the starting material (Scheme 2). First, we adopted palladium-catalyzed Sonogashira coupling with 1-hexadecyne following a transition-metal-catalyzed hydrogenation reaction to introduce the hexadecyl chain, which

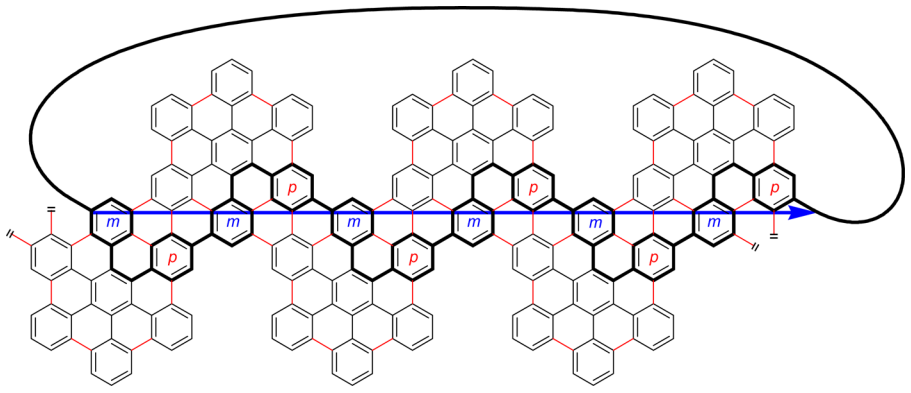

Figure 5. Zigzag-type CNT segment presumed to result from the cyclodehydrogenation reaction of cyclic compound **2**. The arrow represents the chiral vector of the segment.

DOI: 10.1021/acs.joc.5b00485
J. Org. Chem. 2015, 80, 5092–5110

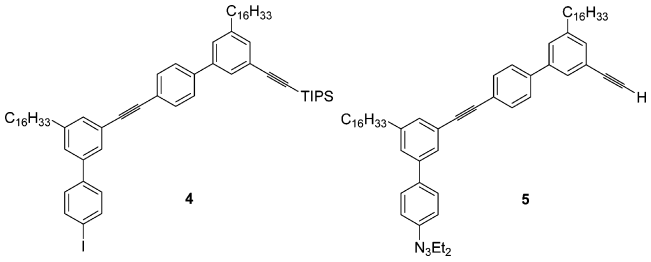

Figure 6. Required building blocks **4** and **5** for the synthesis of the cyclic biphenylylene–acetylene derivative **1**.

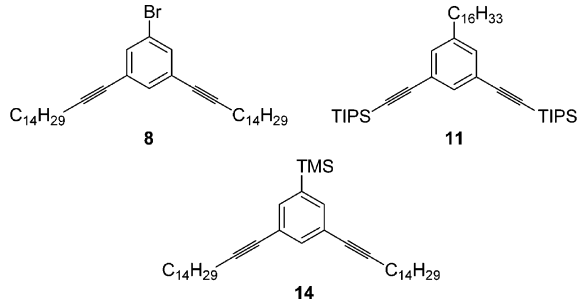

Figure 7. Byproducts obtained by multiple Sonogashira coupling reactions of 1-hexadecyne and TIPS acetylene.

prevents low solubility during the synthetic procedure. Thus, compound **6** was reacted with 1-hexadecyne under palladium-catalyzed Sonogashira coupling conditions. The selectivity of the reaction was not superior, but the desired monosubstituted product **7** was obtained in 68% yield along with the bis-substituted product **8** in 16% yield (Figure 7). The separation of the products was easily established by gel permeation chromatography (GPC) with chloroform as the eluent. Catalytic hydrogenation was effectively established without the unfavorable reductive debromination reaction by utilizing PtO_2 as a catalyst in THF in almost quantitative yield. Introduction of a triisopropylsilylacetylene (TIPS acetylene) unit, which should tolerate the subsequent Suzuki–Miyaura cross-coupling reaction into dibromide **9**, was established by utilizing a Sonogashira coupling reaction. However, the selectivity of the reaction between the mono- and bis-substituted products **10** (55%) and **11** (12%) was still insufficient, although the reactive position was reduced by comparison with starting the Sonogashira coupling reaction with **6**.

To reduce the reactive positions in the Sonogashira coupling reaction, the preparation commenced with 3,5-dibromophenyltrimethylsilane (**12**), which was obtained from **6** through a monolithiation and trimethylsilylation sequence with TMSCl.[18] Although the first Sonogashira coupling reaction still has two reactive positions, in the improved scheme (Scheme 2), the second Sonogashira coupling reaction should exhibit high selectivity because of the difference in reactivity between the two halogen atoms. Thus, the first Sonogashira coupling reaction was established to afford the desired monosubstituted product **13** in 70% yield together with bis-substituted product **14** in 8.6% yield (Figure 7). Catalytic hydrogenation of **13** was also effectively established by utilizing PtO_2 as a catalyst in THF in almost quantitative yield. The trimethylsilyl group of **15** was transformed into an iodo substituent by reaction with ICl in dichloromethane at −55 °C in quantitative yield. This reaction is generally established by heating with ICl in carbon tetrachloride, but, in this case, the heating resulted in contamination with an unexpected and inseparable chlorination product.[19] Introduction of TIPS acetylene by Sonogashira coupling into bromoiodobenzene **16** was selectively established without formation of the bis-substituted product.

Preparation of the two building blocks, **4** and **5**, from **10** is represented in Scheme 3. [(4′-Amino-5-hexadecylbiphenyl-3-yl)ethynyl]triisopropylsilane (**17**) was obtained by a Suzuki–Miyaura cross-coupling reaction of **10** with 4-(4,4,5,5-tetramethyl-1,3,2-dioxaborolan-2-yl)aniline in the presence of $Pd(PPh_3)_4$ as a catalyst in 89% yield. Aminobiphenyl derivative **17** was transformed into 3,3-diethyltriazene **18** by diazotization utilizing isoamyl nitrite followed by treatment with diethylamine in 88% yield. From 3,3-diethyltriazene **18**, both iodide **19** and terminal alkyne **20** were prepared by reaction with iodomethane or tetrabutylammonium fluoride (TBAF) in THF in 97% yield.

When the reaction of iodide **19** was carried out with terminal alkyne **20** divided in several portions (to keep the concentration low in the presence of palladium catalyst), the Sonogashira coupling reaction of **19** with **20** was accomplished in refluxing THF in very high yield (**21**; 95%). From 3,3-

Scheme 2. Two Independent Routes to [(3-Bromo-5-hexadecylphenyl)ethynyl]triisopropylsilane (10)[a]

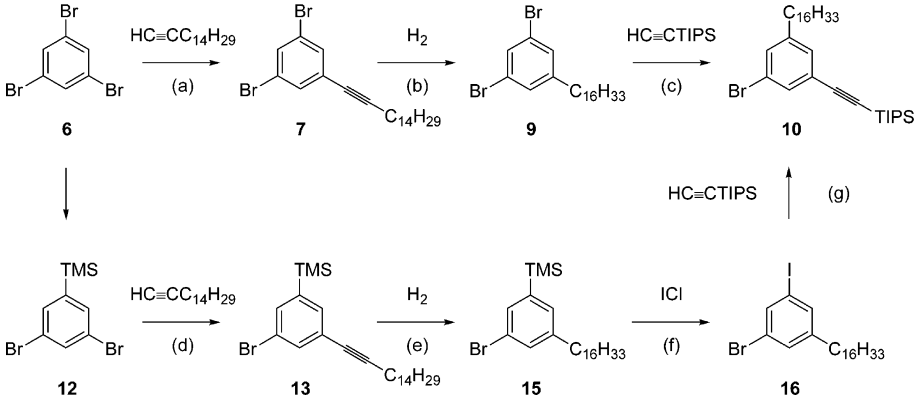

[a]Reagents and conditions: (a) $Pd(PPh_3)_4$, CuI, Et_3N, THF, 60 °C, 5 h, 68%; (b) PtO_2, THF, RT, 18 h, 97%; (c) $PdCl_2(PPh_3)_2$, CuI, Et_3N, THF, 60 °C, 4 h, 55%; (d) $Pd(PPh_3)_4$, CuI, Et_3N, THF, 60 °C, 4 h, 70%; (e) PtO_2, THF, RT, 20 h, 97%; (f) CH_2Cl_2, −55 °C, 4 h, quant.; (g) $PdCl_2(PPh_3)_2$, CuI, Et_3N, THF, 50 °C, 4 h, 96%.

DOI: 10.1021/acs.joc.5b00485
J. Org. Chem. 2015, 80, 5092−5110

Scheme 3. Preparation of the Biphenyl Dimers 4 and 5[a]

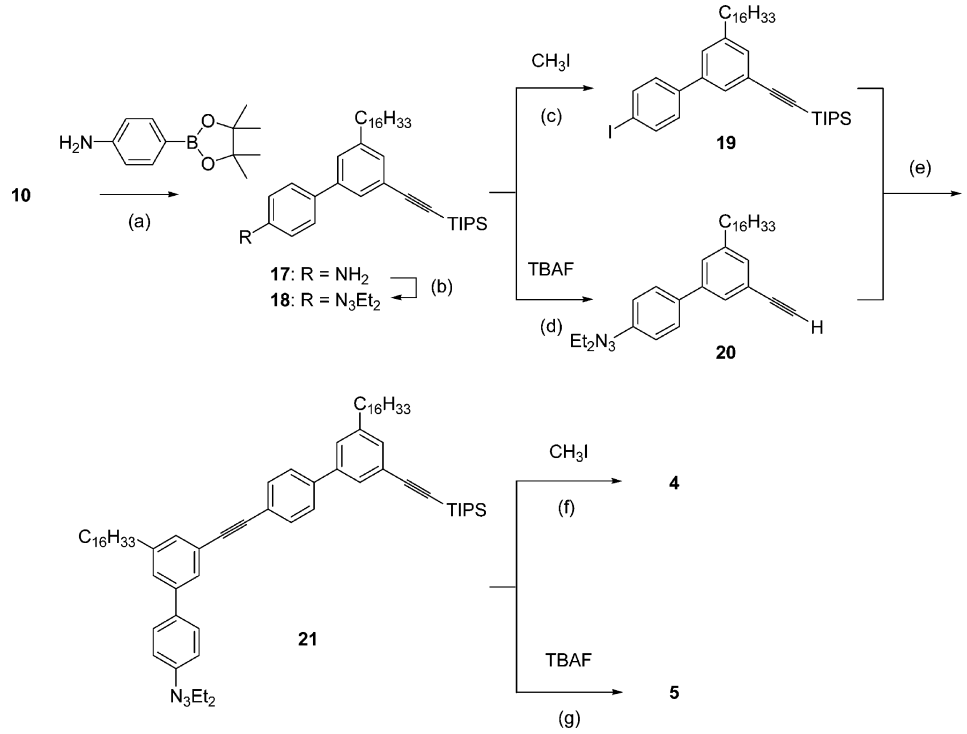

[a]Reagents and conditions: (a) $Pd(PPh_3)_4$, Na_2CO_3 aq., toluene, reflux, 24 h, 89%; (b) (1) $BF_3{\cdot}OEt_2$, $C_5H_{11}ONO$, −15 °C, 0.5 h, (2) Et_2NH, K_2CO_3, 0 °C, 2 h, 88%; (c) 120 °C [in autoclave], 24 h, 97%; (d) THF, RT, 4 h, 97%; (e) $Pd(PPh_3)_4$, CuI, Et_3N, THF, reflux, 4 h, 95%; (f) 120 °C [in autoclave], 1.5 days, 98%; (g) THF, RT, 1 h, 92%.

diethyltriazene **21**, two products, iodide **4** and terminal alkyne **5**, were prepared by reaction with iodomethane or TBAF in THF in 98 and 92% yields, respectively.

Scheme 4 summarizes the preparation of cyclic polyphenylene array **2** from key precursors **4** and **5**. When the reaction of iodide **4** was carried out by keeping the concentration of terminal alkyne **5** low, the Sonogashira coupling reaction of **4** with **5** was accomplished in refluxing THF in 88% yield. 3,3-Diethyltriazene **22** was transformed into iodide **23** by reaction with iodomethane in 99% yield.

Biphenyl hexamer **24** was obtained by the Sonogashira coupling reaction of **23** with **5** in refluxing THF in 74% yield by keeping the concentration of the terminal alkyne **5** low. 3,3-Diethyltriazene **24** was transformed into iodide **25** by reaction with iodomethane in 98% yield; treatment of **25** with TBAF in THF afforded the presumed precursor for cyclic biphenylylene−acetylene derivative **1** in 98% yield. The preparation of precursor **26** takes 16 steps from **12**, but the yield of most of the reaction was over 80%. Thus, the total yield of precursor **26** was 28% in 16 steps from **12**.

We have examined the intramolecular Sonogashira coupling reaction of acyclic biphenyl hexamer **26** by keeping the concentration of **26** low in the presence of palladium catalyst. Thus, compound **1** was obtained in 44% yield, along with the recovery of **26**, when the intramolecular Sonogashira coupling reaction was carried out in a refluxing mixed solvent of Et_3N and toluene for 12 h. The yield of **1** was slightly improved by prolonged heating for 26 h, 48% yield, without the recovery of **26**. Elevating the reaction temperature by changing the base to *N*,*N*-diisopropylethylamine (DIPEA) instead of triethylamine significantly improved the yield of cyclization product **1** to 68% (Table 1).

Cyclic compound **2** was obtained by a 6-fold Diels−Alder reaction of **1** with **3** in a single-step reaction. A high concentration was required for the success of the Diels−Alder reaction, but the homogeneity of the viscous reaction mixture was also important. To improve the homogeneity, **1** and **3** were first mixed by dissolving them into the appropriate amount of THF. After the solvent was removed in vacuo, to the well-combined mixture were added a small amount of diphenylether and THF. The combined mixture was stirred at 200−220 °C for 15 h under an Ar atmosphere. The volatile THF should be vaporized in the reaction vessel by increasing the reaction temperature. Column chromatography on silica gel (dichloromethane/hexane) and GPC (chloroform) of the reaction mixture afforded **2** in 86% yield as a pale yellow powder, which included a small amount of penta-addition product that could be characterized by MALDI-TOF MS measurement. The isolation of **2** was accomplished by subsequent column chromatography on silica gel with dichloromethane/hexane (2:3) as pale yellow crystals. To our knowledge, this is the first example of a cyclic polyphenylene array with the carbon skeleton of a zigzag-type CNT segment, although a multistep reaction was required to attain the product. The spectral features of the new products are in agreement with the structure of the products as summarized in the Experimental Section.

To accomplish an easy synthesis of **1**, we have examined the shotgun synthesis of **1** from 3-ethynyl-4′-iodo-5-hexadecylbiphenyl (**27**), which was prepared by deprotection of the TIPS group from **19** in 91% yield (Scheme 5). However, the one-pot synthesis of **1** from **27** resulted in the formation of an unidentified mixture, probably due to the formation of the oligomers of **27**.

DOI: 10.1021/acs.joc.5b00485
J. Org. Chem. 2015, 80, 5092−5110

Scheme 4. Preparation of Cyclic Polyphenylene Array 2 for the Zigzag-Type CNT Segment with (18,0)-Structure[a]

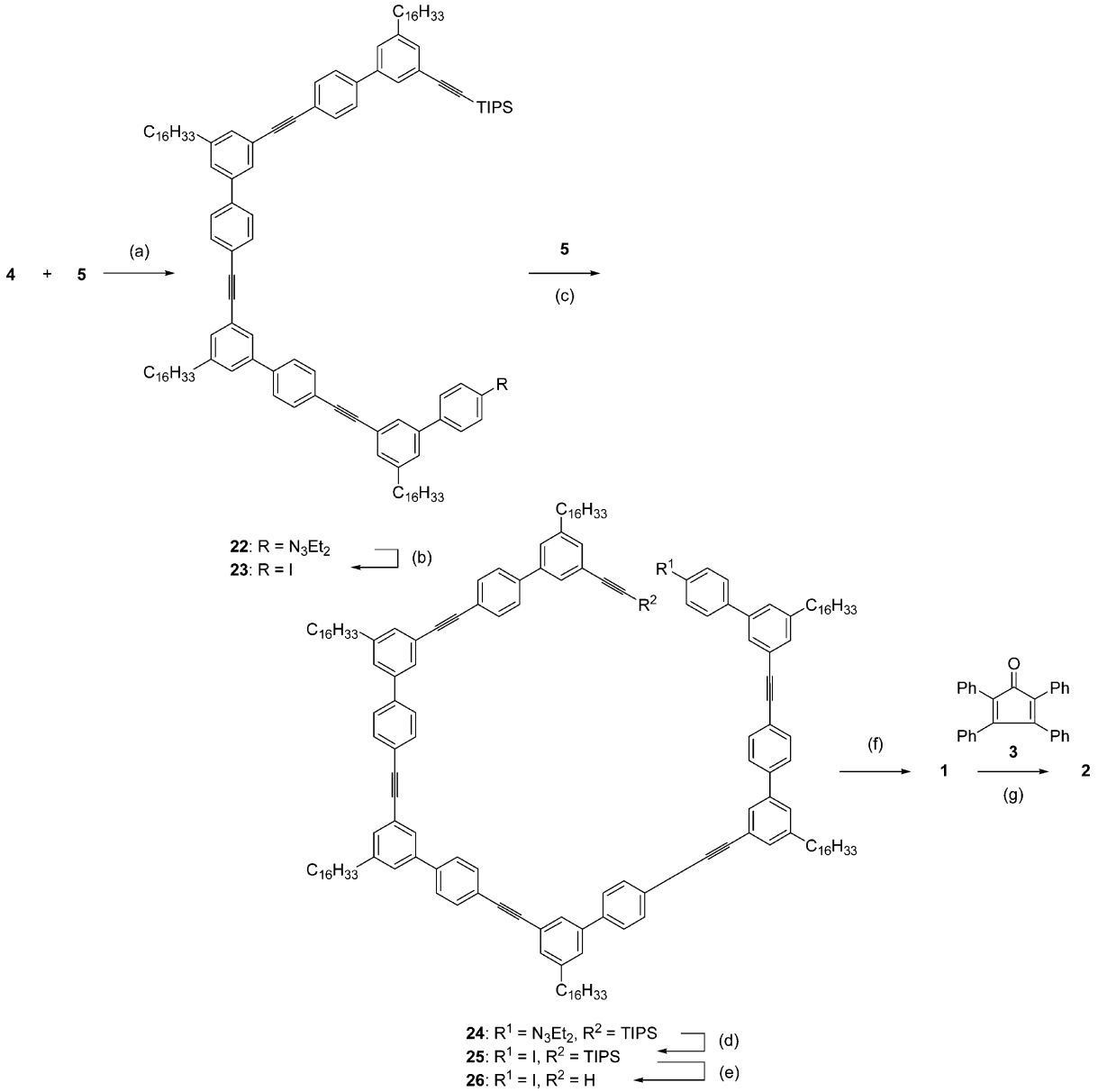

[a]Reagents and conditions: (a) $Pd(PPh_3)_4$, CuI, Et_3N, THF, reflux, 5 h, 88%; (b) CH_3I, 120 °C [in autoclave], 2 days, 99%; (c) $Pd(PPh_3)_4$, CuI, Et_3N, THF, reflux, 5 h, 74%; (d) CH_3I, 120 °C [in autoclave], 1.5 days, 98%; (e) TBAF, THF, RT, 1.5 h, 98%; (f) $Pd(PPh_3)_4$, CuI, base, toluene, reflux (for details, see Table 1); (g) diphenyl ether, 200–220 °C, 15 h, 86%.

Table 1. Intramolecular Sonogashira Coupling Reaction of 26 in a Refluxing Mixed Solvent of Base and Toluene

entry	base	time (h)	yield (%)
1	Et_3N	12	44
2	Et_3N	26	48
3	DIPEA	24	68

Scheme 5. Attempt To Construct the Cyclization Product 1 by Shotgun Synthesis from 27

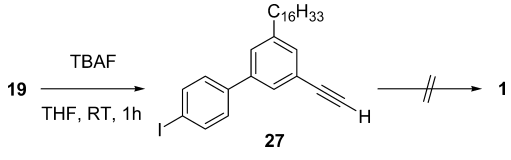

Spectroscopic Properties. All new compounds reported were fully characterized by spectroscopic methods, which afford insight into the structure of these compounds (see the Experimental Section). The NMR spectra of all new products in $CDCl_3$ are summarized in the Supporting Information, which are consistent with the structure of the products.

^1H NMR spectra of **1** and acyclic biphenyl hexamer **26** measured at 500 MHz in $CDCl_3$ are shown in Figures S62 and S60, respectively (see the Supporting Information). Comparison of the ^1H NMR spectrum of **1** with that of **26** revealed the highly symmetrical structure of macrocycle **1**. The disappearance of the terminal acetylenic proton at 3.09 ppm and the typical doublet signal for the aromatic protons adjacent to iodine at 7.77 and 7.35 ppm also fulfills a criterion for the formation of the cyclic biphenylylene–acetylene structure. The broad signals observed in the ^1H NMR spectrum of **2** at 6.4–

DOI: 10.1021/acs.joc.5b00485
J. Org. Chem. 2015, 80, 5092–5110

6.9 and 0.9−2.2 ppm for aromatic and alkyl protons, respectively, were in agreement with a polyphenylene structure having a considerably high molecular weight.

MALDI-TOF MS analysis should afford a valuable characterization of the oligomeric structure of the reaction products. We examined the MALDI-TOF MS measurements using dithranol as a matrix that was calibrated by the ion peaks of polypropylene glycol measured under the same conditions. The results of the measurements are summarized in the Experimental Section. Silver trifluoroacetate was a better auxiliary agent in the MALDI-TOF MS measurements to obtain the correct molecular ion peaks for the high molecular weight carbon-rich materials. In most cases, correct molecular ion peaks were obtained as $[M + Ag]^+$ ion peaks when the measurement was carried out with silver trifluoroacetate. Simulated isotopic signal patterns exhibit good agreement with the observed molecular ion peaks of these high molecular weight compounds, as shown in Figures 8 and 9 for **1** and **2**,

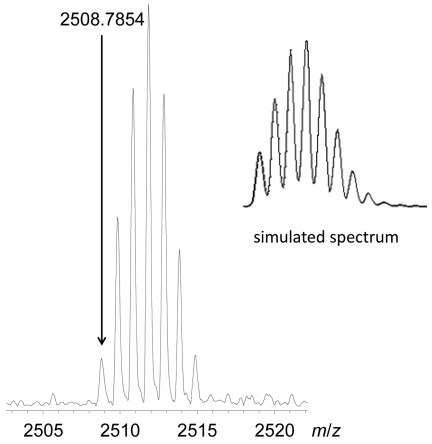

Figure 8. MALDI-TOF MS of **1** measured with silver trifluoroacetate as an auxiliary agent with the simulated isotropic signal pattern of $[M + Ag]^+$ (inset).

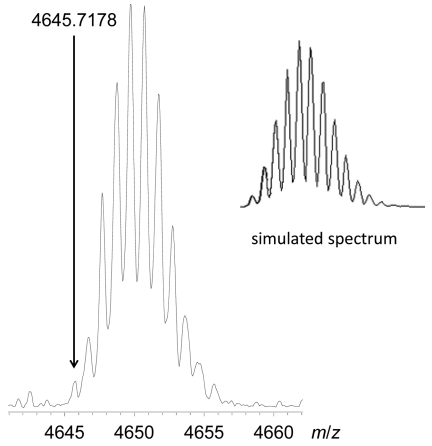

Figure 9. MALDI-TOF MS of **2** measured with silver trifluoroacetate as an auxiliary agent with the simulated isotropic signal pattern of $[M + Ag]^+$ (inset).

respectively. The full-range spectrum of cyclic compound **2** is represented in Figure S66 (see the Supporting Information), which may provide a criterion indicating unity in the final product. GPC analysis of isolated **2**, performed by using recycling techniques in Figure S67 (see the Supporting Information), also affords evidence for the purity of the product, although clear NMR signals of **2** were not obtained, probably due to the high molecular weight of the cyclic polyphenylene derivative.

Acyclic biphenyl hexamer **26** with a terminal alkyne also required the addition of silver trifluoroacetate as an auxiliary agent to obtain molecular ion peaks, but they were observed as $[M - H + 2Ag]^+$ in the MALDI-TOF MS measurement. Iodobiphenyl **27**, prepared for shotgun synthesis, also showed a similar tendency. These results are explained by the formation a silver acetylide with the auxiliary agent that should be ionized with another silver ion to afford the molecular ion peaks.

Other features appeared in the MALDI-TOF MS of the rather high molecular weight material having a *N*,*N*-diethyltriazene function. Biphenyl hexamer **24** with an *N*,*N*-diethyltriazene function was ionized as $[M - N_3Et_2 + H + Ag]^+$ ion peaks when the measurement was carried out with silver trifluoroacetate as an auxiliary agent. These results indicate that the detachment of the *N*,*N*-diethyltriazene function by laser irradiation resulted in its replacement by a hydrogen atom that was ionized by the silver agent. In the series of small molecules with a *N*,*N*-diethyltriazene function, up to biphenyl tetramer **22** could be ionized as $[M + H]^+$ without the addition of the auxiliary agent. These results indicate that MALDI-TOF MS measurement is a useful choice for the characterization of the rather high molecular weight materials investigated in this research.

UV/vis and fluorescence (FL) spectra of **1** and **2** in several solvents are shown in Figures 10 and 11. Compound **1** showed a characteristic absorption band in the UV/vis spectrum at λ_{max} = 312 nm (log ε 5.41) that is consistent with the biphenylylene−acetylene structure of this compound without significant steric hindrance. Intense FL of **1** was observed at λ_{FL} = 351 and 368 nm. The small Stokes shift (39 nm) is consistent with the rigid cyclic structure of **1**. The longest absorption maximum of **2** on the UV/vis spectra [λ_{max} = 254 nm (log ε 5.41)] exhibits a blue shift by 58 nm relative to that of **1**. FL of **2** was observed at λ_{FL} = 374 nm with a large Stokes shift (120 nm) that can be explained by the flexible structure of **2**. Table 2 summarizes the optical properties of **1** and **2**.

Compounds **1** and **2** also showed rather efficient blue emission in the solid state. FL emission in the solid state, observed by excitation resulting from irradiation with a black light, is represented in Figure 12. Thus, we have investigated FL quantum efficiencies (Φ_{FL}) and lifetimes (τ_{FL}) of **1** and **2** in dichloromethane solution and in the crystalline state to gain further insight into the photophysical properties of these molecules. The absorption and FL spectra of powdered **1** and **2** are shown in the Supporting Information.

In the solid-state, characteristic FL of **1** was observed at λ_{FL} = 423 nm by excitation at λ_{AB} = 312 nm, with the absorption maximum in solution showing a red shift by 72 nm. The excitation spectrum of **1** (λ_{EX} = 368 nm) in the solid state at λ_{FL} = 423 nm showed a remarkable red shift (λ_{EX} = 368 nm) of 56 nm relative to the absorption maximum in solution. However, there is little dependence in the FL maximum on the excitation at the maximum (λ_{EX} = 368 nm) in **1**, but the excitation varies the intensity of the FL. An increase in the Stokes shift (55 nm) may be concluded due to intramolecular interactions occurring in the condensed state, such as J-aggregation.

The FL maximum of **2** in the solid state was observed at λ_{FL} = 374 nm, which is the same as that in dichloromethane solution when the excitation was carried out at the absorption

DOI: 10.1021/acs.joc.5b00485
J. Org. Chem. 2015, 80, 5092−5110

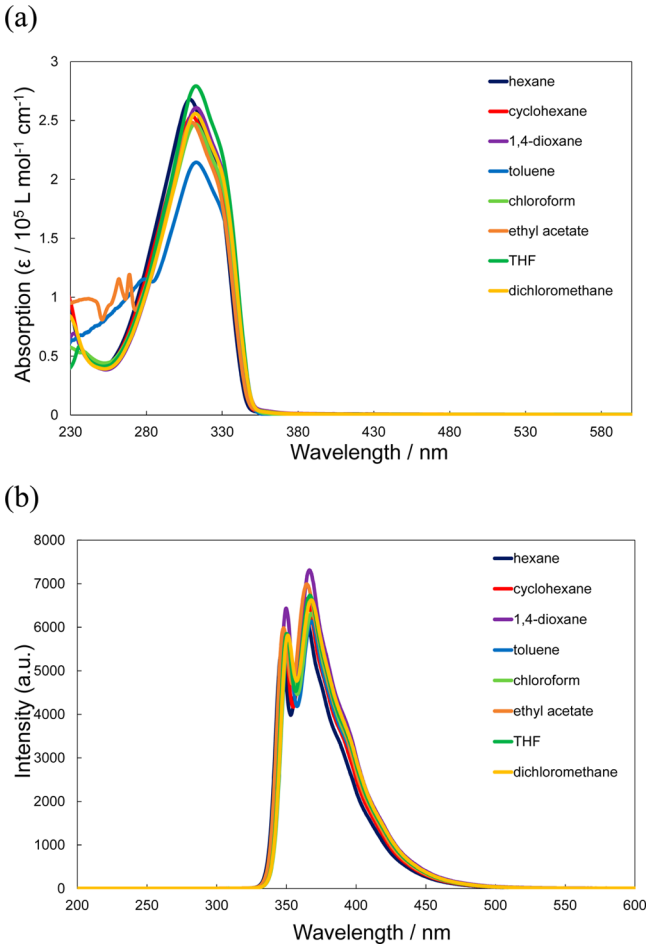

Figure 10. (a) UV/vis and (b) FL spectra of **1** in several solvents (λ_{EX} = 312 nm).

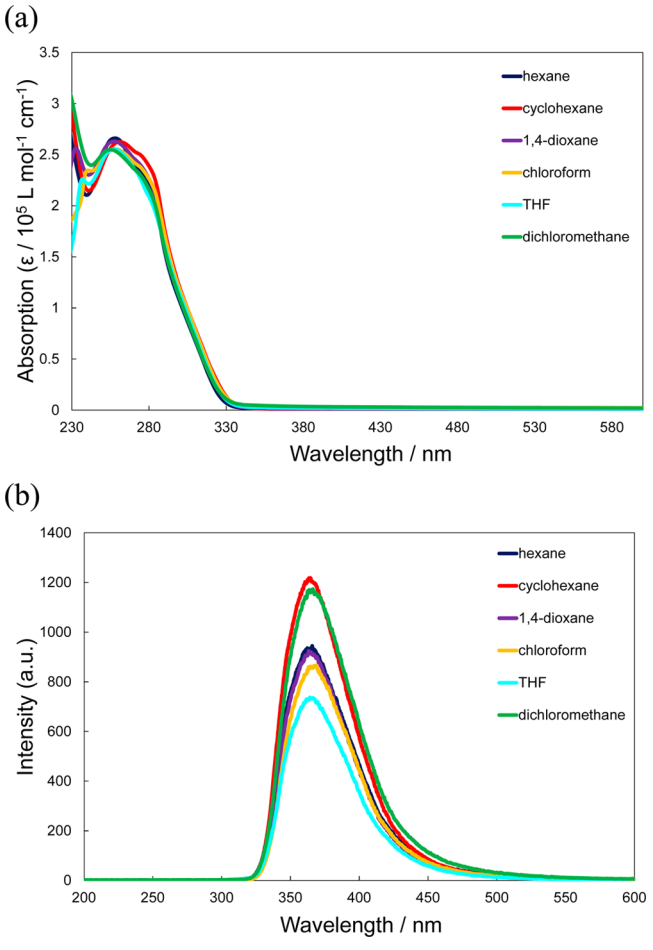

Figure 11. (a) UV/vis and (b) FL spectra of **2** in several solvents (λ_{EX} = 254 nm).

maximum (λ_{AB} = 254 nm). The excitation spectrum in the solid state at λ_{FL} = 374 nm showed a remarkable red shift (λ_{EX} = 333 nm) by 79 nm relative to that in solution. However, there is little dependence of the FL maximum on the excitation of **2** at the maximum (λ_{EX} = 333 nm) in the solid state, but the excitation varies the intensity of the FL. That the same FL maximum in the solid state was observed in solution may be caused by alternation in the absorption transition or emission from an excited state formed by the transition, such as a J-aggregate.

Φ_{FL} in dichloromethane was determined to be 0.56 for **1** (4.66×10^{-6} M). The rather high Φ_{FL} in the solution should be attributed to the rigid cyclic structure of **1**. Substrate **1** still showed a rather high Φ_{FL} (0.29) in the solid state, but it showed a somewhat low Φ_{FL} relative to that in solution, probably due to the effects of intermolecular interaction in the condensed state. Thus, a small change in Φ_{FL} from 0.61 to 0.63 at 1.17 and 2.33×10^{-6} M, respectively, upon dilution is not inconsistent with the conclusion.

Φ_{FL} of **2** showed a slight increase in the solid state (Φ_{FL} = 0.18) compared with that in solution (Φ_{FL} = 0.13). The FL efficiency is quenched in the condensed state by intermolecular interactions. The FL efficiency in **2** is likely due to its tendency to form an amorphos solid in the condensed state, which should affect the quenching of the intermolecular interactions.

To determine τ_{FL}, the time profile for the FL decay of **1** was analyzed by monitoring several FL wavelengths, λ_{FL} = 351, 368, 380, 400, and 420 nm (λ_{EX} = 295 nm), in dichloromethane solution at 298 K (Figure 13). In solution, **1** was characterized as τ_{FL} = 0.76 ns (100% contribution) at FL peak 1 by CHISQ analysis. Luminescence with a little longer lifetime of τ_{FL} = 2−4 ns was observed in the longer-wavelength region, but the contribution was less than 10% (see the Supporting Information).

In the solid state, the contribution of the longer-lifetime species increased in the FL decay, which was characterized as three components by CHISQ analysis of the FL peak (423 nm): τ_{FL} = 0.88 (15%), 2.64 (62%), and 7.24 ns (23%) (λ_{EX} = 371 nm). The FL decay profile of **1** in the solid state was also monitored at λ_{FL} = 400 and 450 nm (λ_{EX} = 295 nm) and showed almost the same tendencies (see the Supporting Information).

Cyclic compound **2** included three components in its FL decay in dichloromethane (Figure 14). The analysis revealed that the major components of the FL decay were species with shorter lifetimes [i.e., τ_{FL} = 0.23 (44%), 0.70 (55%), and 3.49 ns (1%)] (λ_{EX} = 295 nm). The contribution of components with longer lifetimes was just a few, but they are essential for the FL decay observed in CHISQ analysis. In the solid state, **2** included a certain contribution of species with longer lifetimes in the FL decay [i.e., τ_{FL} = 0.72 (63%), 2.01 (22%), and 16.85 ns (15%)] (λ_{EX} = 295 nm).

Thus, the larger contribution of longer-lifetime species in the FL decay in the solid state relative to that in dichloromethane

DOI: 10.1021/acs.joc.5b00485
J. Org. Chem. 2015, 80, 5092−5110

Table 2. Optical Properties of 1 and 2 in Dichloromethane and in the Solid State at 298 K

	CH_2Cl_2 solution					solid state				
	λ_{AB}	λ_{FL}	Stokes shift	τ_{FL}	Φ_{FL}	λ_{EX}	λ_{FL}	Stokes shift	τ_{FL}	Φ_{FL}
sample	nm	nm	nm	ns (%)		nm	nm	nm	ns (%)	
1	312	351	39	0.76 (100)	0.56	368	423	55	0.89 (15)	0.29
		368							2.64 (62)	
									7.24 (23)	
2	254	374	120	0.23 (44)	0.13	333	374	41	0.72 (63)	0.18
				0.70 (55)					2.01 (22)	
				3.49 (1)					16.85 (15)	

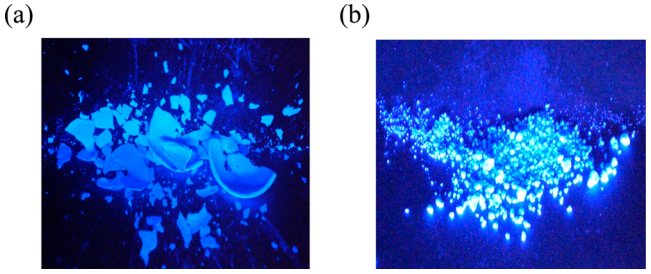

Figure 12. Solid-state FL of (a) **1** and (b) **2**.

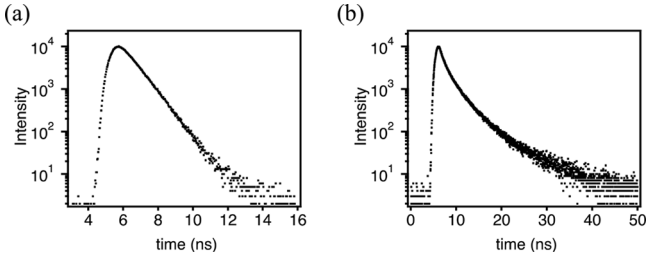

Figure 13. FL decay profile of **1** (a) in dichloromethane (λ_{FL} = 351 nm) and (b) in the solid state (λ_{FL} = 423 nm) at 298 K.

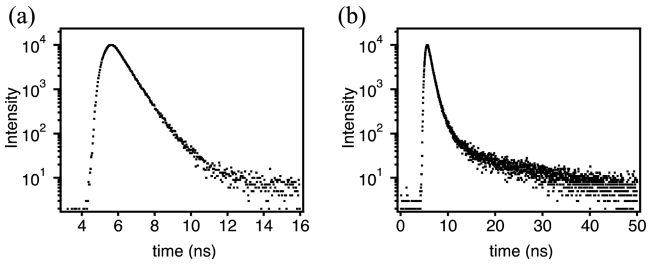

Figure 14. FL decay profile of **2** (a) in dichloromethane (λ_{FL} = 374 nm) and (b) in the solid state (λ_{FL} = 374 nm) at 298 K.

may be consistent with intermolecular interactions in the condensed state of cyclic compounds **1** and **2**, such as J-aggregation.

The solvent dependence of the UV/vis and FL spectra of **1** and **2** in several solvents was also examined (Figures 10 and 11). The solvent dependence of the Φ_{FL} of **1** and **2** are summarized in Tables 3 and 4. The Φ_{FL} of **1** and **2** varies from 0.49 to 0.62 and from 0.09 to 0.13, respectively, relative to their Φ_{FL} in dichloromethane. The small solvent effect may be induced by their hydrocarbon structure.

Theoretical Calculations. To better understand the electronic properties of **1**, we performed time-dependent density functional theory (DFT) calculations at the B3LYP/6-31G* level of the model compound without six hexadecyl

Table 3. Solvent Dependence of the UV/Vis and FL Spectra of 1

solvent	λ_{AB} (nm)	λ_{FL} (nm)		Stokes shift (nm)	Φ_{FL}[a]
hexane	309	347	363	38	0.49
cyclohexane	310	348	365	38	0.54
1,4-dioxane	313	350	367	37	0.59
toluene	313	351	368	38	0.62
chloroform	312	351	368	39	0.55
ethyl acetate	310	348	365	38	0.60
THF	313	350	367	37	0.51

[a]Relative to the absolute Φ_{FL} measured in dichloromethane.

Table 4. Solvent Dependence of the UV/Vis and FL Spectra of 2

solvent	λ_{AB} (nm)	λ_{FL} (nm)	Stokes shift (nm)	Φ_{FL}[a]
hexane	258	366	108	0.10
cyclohexane	261	364	103	0.13
1,4-dioxane	257	364	107	0.09
chloroform	258	369	111	0.09
THF	258	364	106	0.08

[a]Relative to the absolute Φ_{FL} measured in dichloromethane.

groups for simplification.[20] The structure was optimized as a symmetrical structure as illustrated in Figure 15a. The core size

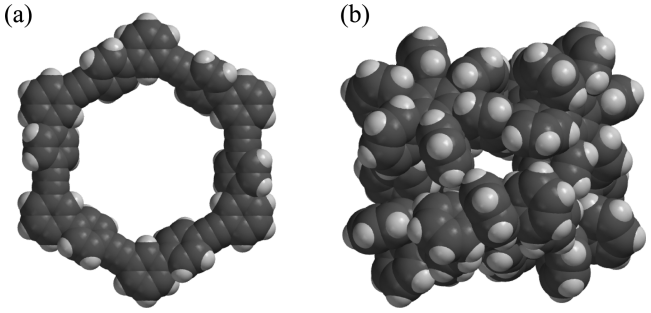

Figure 15. Optimized structures of **1** (DFT B3LYP/6-31G* level) and **2** (HF 3-21G level) without six hexadecyl groups: (a) **1** without six hexadecyl groups and (b) **2** without six hexadecyl groups.

of the molecule was calculated to be 24.2 Å (distance between the carbon atoms of the edges). Molecular modeling of **1** at the molecular mechanics level revealed that the total molecular size, i.e., distance between the terminal carbon atoms of the hexadecyl groups, is 59.2 Å. The time-dependent (TD)-DFT calculations reproduced the red shift in the longest wavelength absorption band of **1**. On the basis of a comparison between the UV/vis (experiment) and electronic transition (theory) spectra, the absorption maxima of **1** could be assigned to a

DOI: 10.1021/acs.joc.5b00485
J. Org. Chem. 2015, 80, 5092−5110

$\pi-\pi^*$ transition that is likely to be responsible for its efficient fluorescent properties. The low HOMO (−5.59 eV) and high LUMO (−1.61 eV) energy levels are consistent with the lack of redox waves observed within the range from 2.4 to −2.4 V via cyclic voltammetry (CV) and differential pulse voltammetry (DPV) of **1**, suggesting that the cyclic biphenylylene−acetylene structure is electrochemically inert.

We also performed Hartree−Fock (HF) calculations at the 3-21G level of model compound of **2** without six hexadecyl groups for simplification. The molecular structure was optimized as a spherical shape with a space in the center, as illustrated in Figure 15b. The results of the calculations are summarized in the Supporting Information. The distance between the terminal carbon atoms of the hexadecyl groups was calculated to be 56.9 Å by molecular modeling at the molecular mechanics level. The lower HOMO level (−7.82 eV) and higher LUMO level (2.96 eV) of **2**, relative to those of **1**, should be attributable to the polyphenylene structure of **2**, which corresponds to the shorter wavelength absorption in the UV/vis spectrum of **2** relative to that of **1**.

Mesomorphic Properties. The phase-transition behavior of **1** and **2** was examined using a polarizing microscope (POM) with a heating plate controlled by a thermoregulator and a differential scanning calorimeter (DSC). The DSC thermograms of these compounds are summarized in the Supporting Information. Phase-transition temperatures and enthalpy changes determined by DSC for **1** and **2** are summarized in Table 5. Powder X-ray diffraction patterns measured with Cu

Table 5. Phase-Transition Temperature (T) and Enthalpy Changes (ΔH) of 1 and 2[a]

sample	Phase[b] $\xrightarrow[[\Delta H\ (\mathrm{kJ\ mol^{-1}})]]{T\ (^\circ\mathrm{C})}$ Phase
1	K $\xrightarrow[[64.4]]{49.6}$ M_1 (Col_h) $\underset{}{\overset{[50.0]^c}{\rightleftharpoons}}$ M_2 $\overset{163.1}{\rightleftharpoons}$ I.L. (150.8)
2	Amorphous solid $\overset{Tg = 131.6}{\rightleftharpoons}$ I.L.

[a]Phase-transition temperature (T) and enthalpy change (ΔH) were determined by DSC. [b]Phase nomenclature: K = crystal, M_1 (Col_h) = hexagonal columnar mesophase, M_2 = unidentified columnar mesophase, I.L. = isotropic liquid. [c]Two peaks were too close to determine the enthalpy changes.

Kα radiation distinguished the phase structure among the mesomorphisms in **1** and **2**. Compound **1** showed mesomorphism, whereas the solid state of **2** was revealed to be an amorphous state. The details are given below.

A schematic of the Gibbs free energy versus temperature ($G-T$) of **1** described by the thermal analyses is illustrated in Figure 16. Photomicrographs in Figure 17 represent consequences of the state changes for **1**.

Compound **1** exhibited a phase transition in the first heating process, as depicted by red arrows in Figure 16. The crystalline phase, denoted K, obtained by the recrystallization of **1** from hexane at room temperature exhibited a phase transition at 49.6 °C to a liquid crystalline phase (M_1 phase). Photo (ii) in Figure 17a represents the change of the green-colored crystals [photo (i) in Figure 17a] under POM observation owing to their transition into the liquid crystalline phase (M_1 phase), which

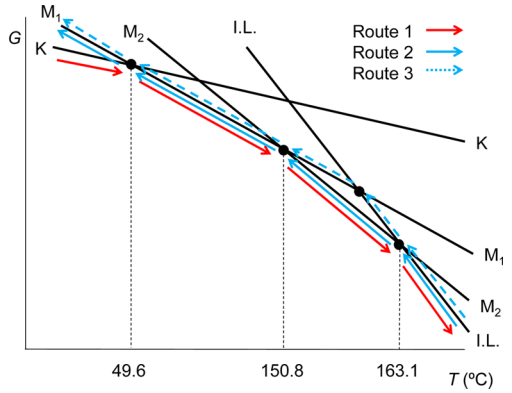

Figure 16. Schematic of the Gibbs free energy versus temperature ($G-T$) of **1** [Route 1 (red arrow), Route 2 (blue arrow), and Route 3 (blue dotted arrow)].

developed an orange color under POM analysis. On further heating, the M_1 phase showed a further phase transition at 150.8 °C to the second liquid crystalline phase (M_2 phase) accompanied by a drastic color change into gray, as shown in photo (iii) in Figure 17a. On further heating, the M_2 phase melted into an isotropic liquid (I.L.) at 163.1 °C (Route 1).

POM observation revealed the existence of two routes in the phase transitions occurring during the cooling process of the I.L. of **1**. The blue arrows in Figure 16 represent one of the phase transitions observed during the cooling process (Route 2). Upon cooling, the gray texture that corresponds to the M_2 phase was first developed [photo (iv) in Figure 17a]. On further cooling, an orange fan-shaped texture that corresponds to the M_1 phase appeared with the gray texture, as shown in photo (v) at 50.0 °C in Figure 17a. Thus, in this route, both M_1 and M_2 phases coexist, which should correspond to their having close energy levels in the two liquid crystalline phases. By the second heating, only the orange fan-shaped texture among the two regions gradually lost its original color at around 156.0 °C [photos (vi) and (vii) in Figure 17a], which changed to the gray texture of the M_2 phase, as shown in photo (viii) at 159.7 °C in Figure 17a. The gray-colored M_2 phase showed a further state change to an I.L. on further heating. Thus, in this route, the phase transition between the M_1 and M_2 states was reversible.

The blue dotted line in Figure 16 demonstrates the other transition route observed in the POM experiments that occurred during the cooling process and featured the direct transition to the M_1 phase from the I.L. of **1**, as shown in Figure 17b (Route 3). The development of the orange fan-shaped texture is unequivocal evidence for the direct transition to the M_1 phase from the I.L. [photos (ix) and (x) in Figure 17b]. By reheating the orange-colored sample, we observed the gradual color change of the M_1 phase into the gray-colored M_2 phase just before the transition to the I.L., as shown in photos (xi), (xii), and (xiii) in Figure 17b.

In most cases, we observed a direct transition to the M_1 phase from the I.L. during the cooling process, as depicted by the blue dotted line in Figure 16 (Route 3). Thus, the texture of the M_2 phase was not reproducible upon POM observation during the cooling process, but the color change attributed to the M_2 phase is reproducible on the reheating process by POM observation. These observations are consistent with the results of the DSC analysis in which the phase transition from the M_1 phase to the M_2 phase was exhibited only on the first heating

DOI: 10.1021/acs.joc.5b00485
J. Org. Chem. 2015, 80, 5092−5110

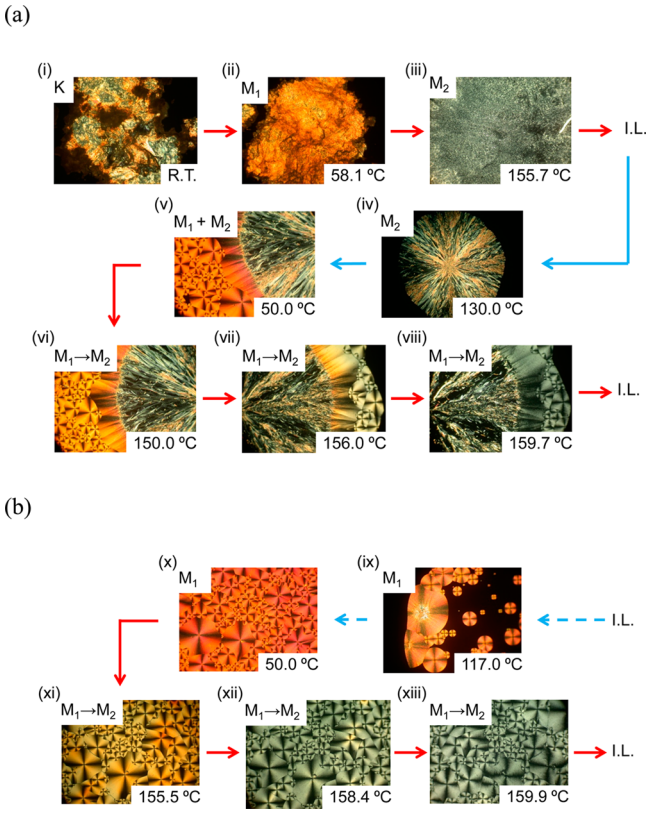

Figure 17. POM images of the mesophase of **1**. (a) Route 1 (red arrow) → Route 2 (blue arrow) → Route 1 (red arrow): (i) textures of **1** obtained by heating from a fresh virgin state obtained by recrystallization from solvent at room temperature; (ii) at 58.1 °C; (iii) at 155.7 °C; (iv) obtained by cooling from the isotropic liquid at 130.0 °C; (v) at 50.0 °C; (vi) by the second heating of the liquid crystalline phase at 150.0 °C; (vii) at 156.0 °C; (viii) at 159.7 °C. (b) Route 3 (blue dotted arrow) → Route 1 (red arrow): (ix) by cooling from the isotropic liquid at 117.0 °C; (x) at 50.0 °C; (xi) by the second heating of the liquid crystalline phase at 155.5 °C; (xii) at 158.4 °C; (xiii) at 159.9 °C.

process (see the Supporting Information). Energy levels in the two states (M_1 and M_2 phases) that are close to each other are responsible for the selection of the state changes that take place from the super cooling of the M_2 state.

The X-ray diffraction experiments revealed the characteristic phase structure of the M_1 state. The pattern at 120 °C that corresponds to the temperature region of the M_1 state is shown in Figure S16 (see the Supporting Information), which exhibits a diffuse band around 2θ = 20° in the wide-angle region, corresponding to the melt of the hexadecyl chains. Compound **1** also gave sharp reflections corresponding to spacings of 19.2, 11.1, and 9.06 Å, and so forth in the small-angle region, which is characteristic of the two-dimensional hexagonal lattice of (100), (110), (200), and so forth, as summarized in Table 6. Thus, the M_1 phase could be identified as a hexagonal columnar structure (Col_h). However, an additional reflection owing to the stacking distance (h) between the disks in the columnar structure could not be identified.

To distinguish the M_2 state, pattern changes were also monitored using X-ray diffraction experiments from 145 to 170 °C in 5 °C intervals. However, we could not obtain clear evidence of the phase structure of the M_2 state. At 145−160 °C, the X-ray diffraction patterns remained close to those of the M_1 phase, whereas at 165 and 170 °C, typical diffraction patterns of

Table 6. X-ray Diffraction Data of the Mesophase of 1 at 120 °C

		spacing (Å)		
sample	mesophase lattice constants (Å)	observed	calculated	Miller indices (*hkl*)
1	Col_h	53.9		H[b]
	a = 22.1 Å	19.2	19.2	(100)
	Z = 1.00 for ρ = 2.00 and h = 4.72 Å[a]	11.1	11.1	(110)
		9.60	9.58	(200)
		7.30	7.24	(210)
		6.41	6.39	(300)
		5.54	5.53	(220)
		4.83	4.79	(400)
		4.43	4.40	(320)

[a]Stacking distances (h = 4.72 Å) in the Col_h phase calculated by the assumption of the number of molecules in a slice (Z = 1.00) and the density of the mesophase (ρ = 2.00 g cm^{-3}). [b]H = presumed helical pitch of the Col_h phase formed by the disc-like structures.

the I.L. were observed. These observations might be explained by the possibility that the M_2 state has a structure that is close to that of the M_1 state. Thus, we have represented the phase as an unidentified liquid crystalline phase (M_2) in Table 5.

The lattice constant of the Col_h phase was calculated as a = 22.1 Å, which corresponds to the core size of the molecule (ca. 25.2 Å) without the long alkyl chains (Figure 15). The large hole in the molecule may be responsible for the rather small lattice constant relative to the large molecular size. This may be rationalized by the intertwining of the molecules to form a Col_h phase that could not be identified as a normal Col phase of the small-sized phenylacetylene macrocycles.[21]

The face-to-face distance of the Col_h phase calculated by assuming the usual number of molecules in the unit cell (Z = 1) also afforded evidence of the unique phase structure of this molecule. In the calculation, an assumption of relatively large density was required to afford the normal face-to-face distance around h = 5 Å. By assuming the density ρ = 2.00 and 1.80 g cm^{-3}, the distance was h = 4.72 and 5.26 Å, respectively. The rather small lattice constant and the requirement of a rather large density to afford the normal face-to-face distance may be an indication of the abnormal phase structure of the Col_h phase, which might be explained by an intertwining of disc-like molecules with a large hole in the center.

In the X-ray diffraction pattern, a broad reflection in the small-angle region depicted by H in Figure S16 that could not be identified as the two-dimensional hexagonal lattice was also observed. The broad reflection (H) suggests the existence of rather long-range order (53.9 Å) in the phase structure. Such one-dimensional regularity has been found in previous work.[22] Thus, the long-range order may be explained by the one-dimensional regularity in which the vertex of the disc-like structure formed by the Col_h structure may describe a helical curve in the mesophase (Figure 18).

To our knowledge, this is the first instance of a columnar mesophase with a large hole in a disc-like compound. The large hole in the molecule may be responsible for the characteristic features of the phase structure of the Col_h phase of **1**.

No mesomorphism was observed in the thermal analyses of **2**. The solid state of **2** obtained by recrystallization from acetone was revealed to be an amorphous solid by utilizing POM observation and powder X-ray diffraction patterns measured with Cu Kα radiation at 110 °C that did not afford

DOI: 10.1021/acs.joc.5b00485
J. Org. Chem. 2015, 80, 5092−5110

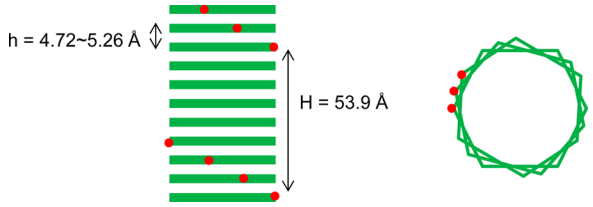

Figure 18. Presumed helical structure of the Col_h phase of **1** formed by its disc-like structure, which is probably due to the intertwining of the molecules with a large hole.

any characteristic reflections but exhibited broad reflections typical of those of an I.L. (see the Supporting Information). The DSC analysis in Figure S15 (see the Supporting Information) revealed the glass transition temperature of the solid to be at 131.6 °C. POM analysis revealed that by heating the white-powdered sample of **2** [photo (a) at room temperature] it exhibited a transition to an I.L. as a clear viscous liquid at 131.6 °C, as can be seen in photo (b) at 150.0 °C in Figure 19. As a result, the solid state of **2** obtained by recrystallization from solvent was revealed to be an amorphous state that exhibits a glass transition to its I.L. at 131.6 °C.

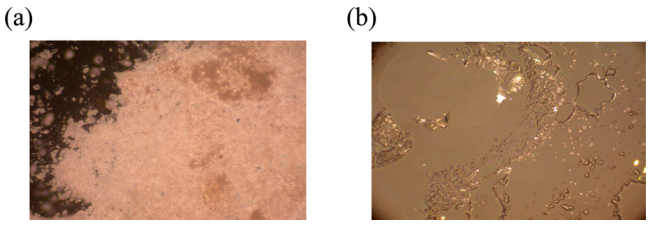

Figure 19. POM images of **2**: (a) white-powdered sample of **2** at room temperature and (b) clear viscous liquid of the I.L. at 150 °C.

Cyclodehydrogenation Reaction. As described above, cyclic polyphenylene array **2** could become a possible precursor for a zigzag-type CNT segment with (18,0)-structure. Elimination of the alkyl chains by a *retro*-Friedel–Crafts reaction or migration to other positions is essential to afford the presumed segment under the highly Lewis acidic cyclodehydrogenation conditions. Using molecular modeling at the HF 3-21G level, we describe a possible tubular structure of the cyclodehydrogenation product of **2** without the six hexadecyl groups, as illustrated in Figure 20.

We examined the cyclodehydrogenation reaction of **2** utilizing excess $FeCl_3$ (630 mol, 6.6 mol per each hydrogen removed) in dichloromethane at room temperature for 3 days, which are the conditions utilized in the cyclodehydrogenation reaction of the cyclic polyphenylene array to afford highly cyclodehydrogenated products. MALDI-TOF MS of the cyclodehydrogenated product of **2** was examined with TCNQ as a matrix, which was calibrated by the ion peaks of polypropylene glycol. The employment of TCNQ as a matrix has been revealed to improve the efficiency of ionization of cyclodehydrogenated products by MALDI-TOF MS measurement.[23] The results of the measurement are presented in Figure 21.

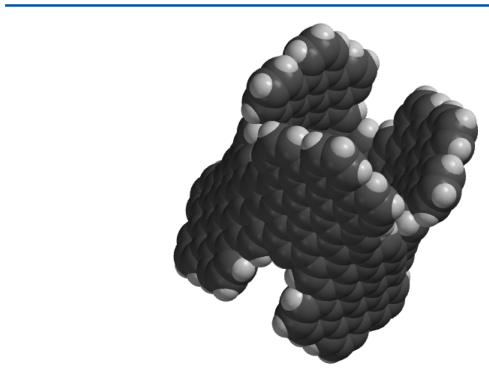

Figure 20. Molecular modeling study on the presumed zigzag-type CNT segment formed from **2**.

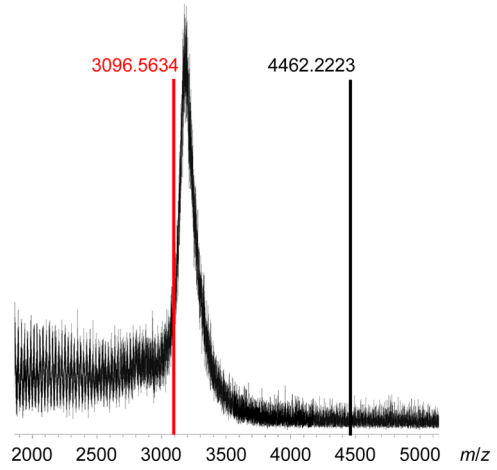

Figure 21. MALDI-TOF MS of the cyclodehydrogenation product of **2** obtained under the typical conditions [matrix: TCNQ]. Red line indicates the mass region of the presumed zigzag-type CNT segment without long alkyl chains, and the black line indicates the mass region of fully cyclodehydrogenated product that retained the long alkyl chains.

MALDI-TOF MS of the cyclodehydrogenated product of **2** revealed the realization of the presumed cyclodehydrogenation and elimination of the alkyl chains under the cyclodehydrogenation conditions. However, broad signals observed in the MS analysis indicated the formation of a complicated mixture of partially dehydrogenated products and/or partially eliminated products about the long alkyl chains. However, the broad signals include the mass region of the presumed zigzag-type CNT segment with (18,0)-structure.

Thus, these results represent the possibility of the formation of the presumed zigzag-type CNT segment. The broad signals might be a result of the severe steric demand in the cyclodehydrogenation step that is also required to avoid the formation of undesirable structurally different congeners, such as a planar structure, as illustrated in Figure 22. The MALDI-TOF MS analysis may be complicated by this problem because a planar structure might afford the same MS number in the molecular ion peaks as those of the presumed zigzag-type CNT segment with (18,0)-structure. Thus, addition of the proper steric demand into the precursor, the cyclic polyphenylene array, might become a task for the future to establish the selectivity of the cyclodehydrogenation step leading to the CNT segment.

■ CONCLUSIONS

We have applied the synthetic procedure for the preparation of HBC derivatives to the preparation of a cyclic polyphenylene

DOI: 10.1021/acs.joc.5b00485
J. Org. Chem. 2015, 80, 5092–5110

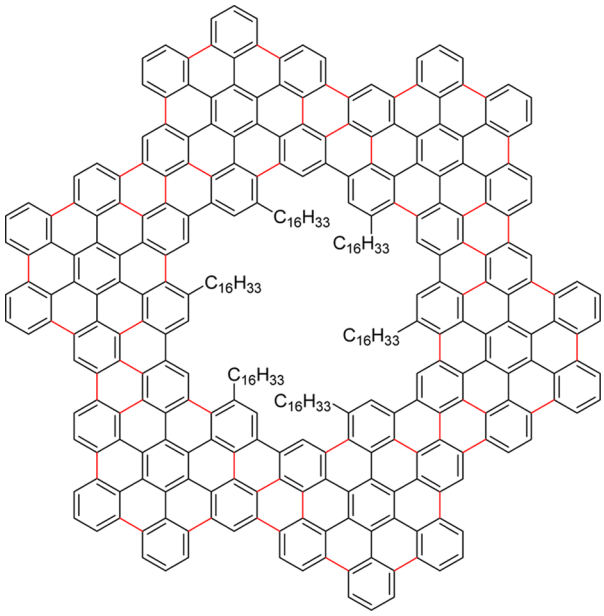

Figure 22. A presumed planar structure of the cyclodehydrogenated product of **2**.

array for a zigzag-type CNT segment with (18,0)-structure. In our approach, we have successfully realized cyclic polyphenylene array **2**, which corresponds to the complete carbon array for a zigzag-type CNT segment (Figure 3) via a Diels–Alder reaction of cyclic biphenylylene–acetylene derivative **1** with tetraphenylcyclopentadienone (**3**). Cyclic polyphenylene array **2** was employed in a cyclodehydrogenation reaction utilizing excess $FeCl_3$ that exhibited the formation of a complicated mixture of partially dehydrogenated products and/or the partially eliminated products about the long alkyl chains, but the mixture included the mass region of the presumed zigzag-type CNT segment with (18,0)-structure.

We have observed several characteristic spectroscopic aspects and thermal behaviors in **1** and **2**. MALDI-TOF MS of the series of new compounds examined in this research measured utilizing silver trifluoroacetate as an auxiliary agent revealed unequivocal evidence for the formation of the cyclic structures.

We have clarified Φ_{FL} and τ_{FL} of **1** and **2** in their crystalline state along with those in a dichloromethane solution. Thus, the larger contribution of the longer-lifetime species in the FL decay in the solid state relative to that in the solution state may be responsible for the rather efficient blue emission of these compounds in the solid state. These results are due to intermolecular interactions in the condensed state of cyclic compounds **1** and **2**, such as J-aggregation.

Thermal analyses of **1** revealed its characteristic phase transition behavior in which the phase structure of **1** with an abnormally small lattice constant in the Col_h phase in spite of its large molecular size was clarified and the solid of **2** was revealed to be an amorphous solid that might be favorable for device fabrication. The large hole in the molecule may be responsible for the characteristic feature in the phase structure of the Col_h phase of **1**.

The synthesis of novel cyclic polyphenylene arrays by a Diels–Alder reaction of cyclic phenylene–acetylene compounds with tetraphenylcyclopentadienone (**3**) may afford attractive precursors for CNT segments. The chemistry for the cyclodehydroganation steps and the synthesis of polyphenylene arrays for the armchair-type and chiral-type CNT segments utilizing this approach are currently under investigation in our laboratory.

EXPERIMENTAL SECTION

General. For general experimental details and the numbering scheme used in the assignment of chemical shifts in NMR experiments, see the Supporting Information.

1,3-Dibromo-5-(hexadec-1-ynyl)benzene (7). To a degassed solution of **6** (1.03 g, 3.27 mmol), CuI (64.2 mg, 0.337 mmol), $Pd(PPh_3)_4$ (197 mg, 0.170 mmol), and triethylamine (15 mL) in THF (20 mL) was added 1-hexadecyne (893 mg, 4.02 mmol) in THF (5 mL) dropwise at 60 °C. The resulting mixture was stirred at the same temperature for 5 h under an Ar atmosphere. The reaction mixture was poured into a 5% NH_4Cl solution and extracted with dichloromethane. The organic layer was washed with a 5% NH_4Cl solution, dried over $MgSO_4$, and concentrated under reduced pressure. The residue was purified by column chromatography on silica gel with hexane and GPC with chloroform to afford **7** (1.02 g, 68%) and 1-bromo-3,5-di(hexadec-1-ynyl)benzene (**8**) (321 mg, 16%).

Compound **7**: colorless crystals; mp 31.4–32.6 °C (hexane); IR (KBr disk): $\tilde{\nu}$ = 3087 (w), 2920 (s), 2849 (s), 2232 (m, C≡C), 1582 (s), 1541 (s), 1465 (s), 1427 (s), 1401 (m), 1380 (w), 1353 (w), 1334 (w), 1311 (w), 1291 (w), 1253 (w), 1241 (w), 1099 (m), 987 (m), 969 (w), 879 (m), 853 (s), 794 (m), 749 (s), 722 (m), 668 (m), 569 (w), 524 (w) cm^{-1}; UV/vis (CH_2Cl_2): λ (log ε) = 228 (3.72), 249 (3.60), 253 sh (3.59), 259 (3.66), 279 sh (2.32), 287 (2.35), 299 sh (2.21) nm; ^1H NMR (500 MHz, $CDCl_3$, rt): δ = 7.56 (t, J = 1.7 Hz, 1H, 2-H), 7.46 (d, J = 1.7 Hz, 2H, 4,6-H), 2.38 (t, J = 7.1 Hz, 2H, 3′-H), 1.58 (tt, J = 7.5, 7.1 Hz, 2H, 4′-H), 1.42 (tt, J = 7.5, 6.7 Hz, 2H, 5′-H), 1.35–1.26 (m, 20H, 6′-15′-H), 0.88 (t, J = 6.9 Hz, 3H, 16′-H); ^{13}C NMR (125 MHz, $CDCl_3$, rt): δ = 133.17 (C-2), 133.04 (C-4,6), 127.55 (C-5), 122.42 (C-1,3), 93.67 (C-2′), 77.95 (C-1′), 31.92 (C-14′), 29.69 (t), 29.68 (t), 29.65 (t, 2C), 29.61 (t), 29.49 (t), 29.35 (t), 29.10 (t), 28.88 (C-5′), 28.44 (C-4′), 22.68 (C-15′), 19.34 (C-3′), 14.11 (C-16′); HR-MALDI-MS (dithranol + CF_3CO_2Ag) m/z calcd for $C_{22}H_{32}Br_2 + Ag^+$ $[M + Ag]^+$ 560.9916, found 560.9920; HR-MALDI-MS (dithranol + CF_3CO_2Na) m/z calcd for $C_{22}H_{32}Br_2 + Na^+$ $[M + Na]^+$ 477.0763, found 477.0787.

Compound **8**: colorless crystals; mp 35.9–36.7 °C (EtOH); IR (KBr disk): $\tilde{\nu}$ = 3078 (w), 2921 (s), 2849 (s), 2236 (m, C≡C), 1587 (s), 1550 (s), 1490 (w), 1466 (s), 1425 (s), 1400 (m), 1376 (w), 1334 (w), 1312 (w), 1287 (m), 1266 (w), 1242 (w), 1193 (w), 1128 (w), 1100 (m), 1083 (w), 1071 (w), 1042 (w), 993 (w), 979 (w), 953 (m), 888 (w), 869 (s), 811 (m), 775 (s), 743 (w), 722 (s), 671 (m), 557 (w), 547 (w), 468 (w), 446 (w) cm^{-1}; UV/vis (CH_2Cl_2): λ (log ε) = 232 sh (4.57), 241 (4.64), 251 sh (4.44), 257 (4.42), 263 sh (4.21), 284 sh (2.51), 292 (2.66), 300 (2.79), 302 sh (2.77), 312 (2.76) nm; ^1H NMR (500 MHz, $CDCl_3$, rt): δ = 7.42 (br. d, J = 1.1 Hz, 2H, 2,6-H), 7.32 (br. t, 1H, 4-H), 2.37 (t, J = 7.1 Hz, 4H, 3′-H), 1.58 (tt, J = 7.5, 7.1 Hz, 4H, 4′-H), 1.42 (tt, J = 7.5, 6.4 Hz, 4H, 5′-H), 1.35–1.26 (m, 40H, 6′-15′-H), 0.88 (t, J = 6.9 Hz, 6H, 16′-H); ^{13}C NMR (125 MHz, $CDCl_3$, rt): δ = 133.30 (C-2,6), 133.16 (C-4), 125.89 (C-3,5), 121.53 (C-1), 92.38 (C-2′), 78.69 (C-1′), 31.92 (C-14′), 29.70 (t), 29.69 (t), 29.66 (t), 29.65 (t), 29.63 (t), 29.51 (t), 29.36 (t), 29.13 (C-5′), 28.88 (t), 28.55 (C-4′), 22.69 (C-15′), 19.34 (C-3′), 14.11 (C-16′); HR-MALDI-MS (dithranol + CF_3CO_2Ag) m/z calcd for $C_{38}H_{61}Br + Ag^+$ $[M + Ag]^+$ 703.3002, found 703.2993.

1,3-Dibromo-5-hexadecylbenzene (9). A mixture of **7** (899 mg, 1.97 mmol) and Pt_2O (4.7 mg, 21 μmol) in THF (10 mL) was stirred at room temperature for 18 h under an H_2 atmosphere. After the Pt catalyst was removed by filtration, the solvent was removed under reduced pressure. The residue was purified by column chromatography on silica gel with hexane to afford **9** (883 mg, 97%). Colorless crystals; mp 39.9–41.4 °C (hexane); IR (KBr disk): $\tilde{\nu}$ = 3071 (w), 2951 (m), 2917 (s), 2847 (s), 1585 (s), 1553 (s), 1488 (s), 1462 (m), 1419 (m), 1377 (w), 1363 (w), 1209 (w), 1110 (m), 1084 (m), 1000 (w), 889 (w), 851 (m), 766 (w), 742 (m), 720 (m), 686 (m), 619 (w) cm^{-1}; UV/vis (CH_2Cl_2): λ (log ε) = 228 (3.77), 264 sh (2.49), 271

DOI: 10.1021/acs.joc.5b00485
J. Org. Chem. 2015, 80, 5092–5110

(2.50), 279 sh (2.31) nm; ^{1}H NMR (500 MHz, $CDCl_3$, rt): δ = 7.47 (br. t, 1H, 2-H), 7.25 (br. d, J = 1.4 Hz, 2H, 4,6-H), 2.54 (t, J = 7.8 Hz, 2H, 1′-H), 1.57 (tt, J = 7.8, 7.1 Hz, 2H, 2′-H), 1.34−1.26 (m, 26H, 3′-15′-H), 0.88 (t, J = 6.9 Hz, 3H, 16′-H); ^{13}C NMR (125 MHz, $CDCl_3$, rt): δ = 146.89 (C-5), 131.26 (C-2), 130.26 (C-4,6), 122.66 (C-1,3), 35.37 (C-1′), 31.92 (C-14′), 31.01 (C-2′), 29.69 (t, 3C), 29.66 (t), 29.65 (t), 29.64 (t), 29.61 (t), 29.49 (t), 29.37 (t), 29.36 (t), 29.11 (t), 22.69 (C-15′), 14.12 (C-16′); HR-MALDI-MS (dithranol + CF_3CO_2Ag) m/z calcd for $C_{22}H_{36}Br_2$ + Ag^+ $[M + Ag]^+$ 565.0229, found 565.0223.

[(3-Bromo-5-hexadecylphenyl)ethynyl]triisopropylsilane (10) from 9. To a degassed solution of **9** (764 mg, 1.66 mmol), CuI (32.9 mg, 0.173 mmol), $PdCl_2(PPh_3)_2$ (60.4 mg, 86.1 μmol), and triethylamine (15 mL) in THF (20 mL) was added TIPS acetylene (450 μL, 2.01 mmol) in THF (5 mL) dropwise at 60 °C. The resulting mixture was stirred at 60 °C for 4 h under an Ar atmosphere. The reaction mixture was poured into a 5% NH_4Cl solution and extracted with dichloromethane. The organic layer was washed with a 5% NH_4Cl solution, dried over $MgSO_4$, and concentrated under reduced pressure. The residue was purified by column chromatography on silica gel with hexane and GPC with chloroform to afford **10** (513 mg, 55%) and {[3-hexadecyl-5-(triisopropylsilylethynyl)phenyl]ethynyl}-triisopropylsilane (**11**) (134 mg, 12%).

Compound **10**: colorless oil; IR (neat): $\tilde{\nu}$ = 2956 (m), 2924 (s), 2853 (s), 2155 (m, C≡C), 1594 (w), 1560 (m), 1460 (s), 1384 (m), 1361 (w), 1250 (w), 1156 (w), 1072 (w), 1015 (w), 996 (w), 920 (w), 882 (m), 860 (w), 830 (w), 681 (m) cm^{-1}; UV/vis (CH_2Cl_2): λ (log ε) = 228 (4.22), 242 sh (4.13), 254 (4.37), 265 (4.36), 289 sh (3.26), 298 sh (3.12) nm; ^{1}H NMR (500 MHz, $CDCl_3$, rt): δ = 7.42 (dd, J = 1.6, 1.6 Hz, 1H, 2-H), 7.27 (dd, J = 1.7, 1.6 Hz, 1H, 4-H), 7.20 (br. dd, 1H, 6-H), 2.53 (t, J = 7.8 Hz, 2H, 1″-H), 1.58 (tt, J = 7.8, 7.2 Hz, 2H, 2″-H), 1.33−1.26 (m, 26H, 3″-15″-H), 1.12 (s, 21H, TIPS), 0.88 (t, J = 6.9 Hz, 3H, 16″-H); ^{13}C NMR (125 MHz, $CDCl_3$, rt): δ = 145.02 (C-5), 131.99 (C-2), 131.56 (C-4), 130.64 (C-6), 125.11 (C-1 or C-3), 121.79 (C-1 or C-3), 105.63 (C-1′), 91.65 (C-2′), 35.43 (C-1″), 31.93 (C-14″), 31.15 (C-2″), 29.70 (t), 29.69 (t, 2C), 29.68 (t), 29.66 (t, 2C), 29.64 (t), 29.54 (t), 29.41 (t), 29.36 (t), 29.22 (C-3″), 22.69 (C-15″), 18.64 (q, TIPS), 14.12 (C-16″), 11.26 (d, TIPS); HR-MALDI-MS (dithranol + CF_3CO_2Ag) m/z calcd for $C_{33}H_{57}BrSi$ + Ag^+ $[M + Ag]^+$ 667.2458, found 667.2474; HR-MALDI-MS (dithranol + CF_3CO_2Na) m/z calcd for $C_{33}H_{57}BrSi$ + Na^+ $[M + Na]^+$ 583.3305, found 583.3252.

Compound **11**: colorless oil; IR (neat): $\tilde{\nu}$ = 2925 (s), 2864 (s), 2155 (m, C≡C), 1586 (m), 1464 (s), 1435 (m), 1383 (w), 1368 (w), 1293 (w), 1244 (w), 1161 (w), 1073 (w), 1017 (w), 996 (m), 978 (m), 919 (w), 883 (s), 725 (w), 677 (s), 552 (w), 501 (w), 463 (w) cm^{-1}; UV/vis (CH_2Cl_2): λ (log ε) = 231 sh (4.47), 245 sh (4.69), 250 (4.72), 257 sh (4.55), 265 (4.54), 269 sh (4.39), 287 sh (2.78), 291 sh (2.81), 295 sh (2.84), 299 (2.94), 303 sh (2.86), 307 (2.85), 312 (2.92) nm; ^{1}H NMR (500 MHz, $CDCl_3$, rt): δ = 7.38 (br. t, 1H, 6-H), 7.22 (br. d, J = 1.1 Hz, 2H, 2,4-H), 2.53 (t, J = 7.8 Hz, 2H, 1″-H), 1.59 (br. tt, 2H, 2″-H), 1.34−1.25 (m, 26H, 3″-15″-H), 1.13 (s, 42H, TIPS), 0.88 (t, J = 6.9 Hz, 3H, 16″-H); ^{13}C NMR (125 MHz, $CDCl_3$, rt): δ = 143.10 (C-3), 132.66 (C-6), 132.03 (C-2,4), 123.49 (C-1,5), 106.47 (C-1′), 90.59 (C-2′), 35.52 (C-1″), 31.94 (C-14″), 31.28 (C-2″), 29.71 (t, 2C), 29.69 (t), 29.67 (t, 2C), 29.59 (t), 29.47 (t), 29.37 (t), 29.35 (t), 22.70 (t, C15″), 18.67 (q, TIPS), 14.12 (q, C16″), 11.32 (d, TIPS); HR-MALDI-MS (dithranol + CF_3CO_2Ag) m/z calcd for $C_{44}H_{78}Si_2$ + Ag^+ $[M + Ag]^+$ 769.4687, found 769.4698; HR-MALDI-MS (dithranol + CF_3CO_2Na) m/z calcd for $C_{44}H_{78}Si_2$ + Na^+ $[M + Na]^+$ 685.5534, found 685.5572.

[3-Bromo-5-(hexadec-1-ynyl)phenyl]trimethylsilane (13). To a degassed solution of **12** (12.4 g, 40.2 mmol), CuI (16.3 mg, 0.856 mmol), $Pd(PPh_3)_4$ (46.5 mg, 0.402 mmol), and triethylamine (50 mL) in THF (150 mL) was added 1-hexadecyne (9.04 g, 40.6 mmol) in THF (10 mL). The resulting mixture was stirred at 60 °C for 4 h under an Ar atmosphere. The reaction mixture was poured into a 5% NH_4Cl solution and extracted with chloroform. The organic layer was washed with a 5% NH_4Cl solution, dried over $MgSO_4$, and concentrated under reduced pressure. The residue was purified by column chromatography on silica gel with hexane and GPC with chloroform to afford **13** (12.6 g, 70%) and [3,5-di(hexadec-1-ynyl)phenyl]trimethylsilane (**14**) (2.05 g, 8.6%).

Compound **13**: colorless oil; IR (neat): $\tilde{\nu}$ = 2956 (m), 2925 (s), 2853 (s), 2225 (w, C≡C), 1577 (w), 1543 (m), 1466 (m), 1387 (m), 1251 (m), 1130 (w), 1105 (w), 862 (s), 839 (s), 754 (m), 683 (w), 625 (w) cm^{-1}; UV/vis (CH_2Cl_2): λ (log ε) = 228 (4.17), 248 (4.14), 251 sh (4.13), 258 (4.17), 280 (2.80), 289 (2.93), 298 (2.88) nm; ^{1}H NMR (500 MHz, $CDCl_3$, rt): δ = 7.51 (dd, J = 1.8, 1.6 Hz, 1H, 2-H or 4-H), 7.48 (dd, J = 1.8, 0.8 Hz, 1H, 6-H), 7.42 (br. dd, 1H, 2-H or 4-H), 2.40 (t, J = 7.1 Hz, 2H, 3′-H), 1.60 (tt, J = 7.6, 7.1 Hz, 2H, 4′-H), 1.43 (tt, J = 7.6, 6.8 Hz, 2H, 5′-H), 1.34−1.26 (m, 20H, 6′-15′-H), 0.88 (t, J = 6.9 Hz, 3H, 16′-H), 0.26 (s, 9H, TMS); ^{13}C NMR (125 MHz, $CDCl_3$, rt): δ = 143.36 (C-1), 134.90 (C-6), 134.76 (C-2 or C-4), 134.43 (C-2 or C-4), 125.61 (C-3), 122.24 (C-5), 91.91 (C-2′), 79.43 (C-1′), 31.92 (C-14′), 29.70 (t), 29.69 (t), 29.67 (t), 29.65 (t), 29.63 (t), 29.52 (t), 29.36 (t), 29.15 (C-5′), 28.94 (t), 28.64 (C-4′), 22.69 (C-15′), 19.40 (C-3′), 14.12 (C-16′), −1.36 (TMS); HR-MALDI-MS (dithranol + CF_3CO_2Ag) m/z calcd for $C_{25}H_{41}BrSi$ + Ag^+ $[M + Ag]^+$ 555.1206, found 555.1200.

Compound **14**: colorless crystals; mp 40.2−40.9 °C (acetone); IR (KBr disk): $\tilde{\nu}$ = 2955 (m), 2919 (s), 2850 (s), 2237 (m, C≡C), 1576 (m), 1471 (s), 1428 (w), 1380 (m), 1317 (w), 1265 (w), 1252 (s), 1133 (s), 1090 (m), 967 (w), 896 (w), 875 (m), 857 (s), 837 (s), 810 (w), 787 (w), 754 (m), 718 (m), 691 (m), 626 (m), 548 (w) cm^{-1}; UV/vis (CH_2Cl_2): λ (log ε) = 231 sh (4.56), 240 (4.64), 250 sh (4.43), 257 (4.39), 264 sh (4.14), 289 (2.68), 297 (2.77), 301 sh (2.71), 305 sh (2.61), 310 (2.63) nm; ^{1}H NMR (500 MHz, $CDCl_3$, rt): δ = 7.41 (br. m, 3H, 2,6-H and 4-H), 2.39 (t, J = 7.1 Hz, 4H, 3′-H), 1.60 (tt, J = 7.6, 7.1 Hz, 4H, 4′-H), 1.44 (tt, J = 7.6, 6.7 Hz, 4H, 5′-H), 1.35−1.26 (m, 40H, 6′-15′-H), 0.89 (t, J = 6.9 Hz, 6H, 16′-H), 0.24 (s, 9H, TMS); ^{13}C NMR (125 MHz, $CDCl_3$, rt): δ = 140.61 (C-1), 135.24 (C-2,6), 134.79 (C-4), 123.51 (C-3), 90.74 (C-2′), 80.19 (C-1′), 31.92 (C-14′), 29.70 (t), 29.68 (t), 29.67 (t), 29.65 (t), 29.64 (t), 29.54 (t), 29.36 (t), 29.17 (C-5′), 28.95 (t), 28.75 (C-4′), 22.69 (C-15′), 19.41 (C-3′), 14.11 (C-16′), −1.33 (TMS); HR-MALDI-MS (dithranol + CF_3CO_2Ag) m/z calcd for $C_{41}H_{70}Si$ + Ag^+ $[M + Ag]^+$ 697.4292, found 697.4317; HR-MALDI-MS (dithranol + CF_3CO_2Na) m/z calcd for $C_{41}H_{70}Si$ + Na^+ $[M + Na]^+$ 613.5139, found 613.5144.

(3-Bromo-5-hexadecylphenyl)trimethylsilane (15). A mixture of **13** (6.00 g, 13.3 mmol) and Pt_2O (32.7 mg, 0.144 mmol) in THF (50 mL) was stirred at room temperature for 20 h under an H_2 atmosphere. After the Pt catalyst was removed by filtration, the solvent was removed under reduced pressure. The residue was purified by column chromatography on silica gel with hexane to afford **15** (5.89 g, 97%). Colorless oil; IR (neat): $\tilde{\nu}$ = 2954 (m), 2925 (s), 2853 (s), 1579 (w), 1553 (m), 1466 (m), 1395 (w), 1249 (m), 1209 (w), 1135 (w), 1109 (w), 896 (w), 837 (s), 753 (m), 720 (w), 690 (w), 627 (w) cm^{-1}; UV/vis (CH_2Cl_2): λ (log ε) = 228 (3.72), 274 (2.66), 281 (2.58) nm; ^{1}H NMR (500 MHz, $CDCl_3$, rt): δ = 7.41 (br. s, 1H, 2-H), 7.30 (br. s, 1H, 4-H or 6-H), 7.20 (br. s, 1H, 4-H or 6-H), 2.56 (t, J = 7.8 Hz, 2H, 1′-H), 1.59 (tt, J = 7.8, 7.0 Hz, 2H, 2′-H), 1.36−1.26 (m, 26H, 3′-15′-H), 0.88 (t, J = 6.9 Hz, 3H, 16′-H), 0.26 (s, 9H, TMS); ^{13}C NMR (125 MHz, $CDCl_3$, rt): δ = 144.63 (C-5), 143.31 (C-1), 133.14 (C-2), 131.83 (C-4 or C-6), 131.69 (C-4 or C-6), 122.72 (C-3), 35.70 (C-1′), 31.92 (C-14′), 31.39 (C-2′), 29.69 (t, 3C), 29.68 (t), 29.66 (t, 2C), 29.65 (t), 29.57 (t), 29.44 (t), 29.36 (t), 29.30 (t), 22.69 (C-15′), 14.11 (C-16′), −1.22 (TMS); HR-MALDI-MS (dithranol + CF_3CO_2Ag) m/z calcd for $C_{25}H_{45}BrSi$ + Ag^+ $[M + Ag]^+$ 559.1519, found 559.1535; HR-MALDI-MS (dithranol + CF_3CO_2Na) m/z calcd for $C_{25}H_{45}BrSi$ + Na^+ $[M + Na]^+$ 475.2366, found 475.2240.

1-Bromo-3-hexadecyl-5-iodobenzene (16). A solution of ICl (2.69 g, 16.6 mmol) was added to a solution of **15** (4.93 g, 10.9 mmol) in dichloromethane (300 mL) at −55 °C. The mixture was allowed to stand at the same temperature for 4 h. The reaction was quenched by the addition of powdered $NaHSO_3$ and then poured into a 10% $NaHSO_3$ solution while the mixture was cold. The organic layer was separated, and the aqueous layer was extracted with dichloromethane. The organic layer was combined, dried over $MgSO_4$, and concentrated under reduced pressure. The residue was purified by column

DOI: 10.1021/acs.joc.5b00485
J. Org. Chem. 2015, 80, 5092−5110

chromatography on silica gel with hexane to afford **16** (5.51 g, quant.). Colorless crystals; mp 43.1−44.2 °C (hexane); IR (KBr disk): $\tilde{\nu}$ = 2954 (w), 2916 (s), 2846 (s), 1578 (w), 1547 (m), 1468 (m), 1454 (w), 1417 (w), 849 (w), 725 (w), 686 (w) cm^{-1}; UV/vis (CH_2Cl_2): λ (log ε) = 230 (4.06), 233 sh (4.05), 267 sh (2.86) nm; ^1H NMR (500 MHz, $CDCl_3$, rt): δ = 7.66 (dd, J = 1.7, 1.6 Hz, 1H, 6-H), 7.45 (br. dd, 1H, 2-H or 4-H), 7.28 (br. dd, 1H, 2-H or 4-H), 2.51 (t, J = 7.8 Hz, 2H, 1′-H), 1.56 (tt, J = 7.8, 7.3 Hz, 2H, 2′-H), 1.32−1.26 (m, 26H, 3′-15′-H), 0.88 (t, J = 6.9 Hz, 3H, 16′-H); ^{13}C NMR (125 MHz, $CDCl_3$, rt): δ = 147.05 (C-3), 136.83 (C-6), 136.18 (C-2 or C-4), 130.93 (C-2 or C-4), 122.71 (C-1), 94.32 (C-5), 35.23 (C-1′), 31.92 (C-14′), 31.04 (C-2′), 29.69 (t), 29.69 (t, 2C), 29.67 (t), 29.65 (t), 29.64 (t), 29.61 (t), 29.49 (t), 29.37 (t), 29.36 (t), 29.12 (C-3′), 22.69 (C-15′), 14.12 (C-16′); HR-MALDI-MS (dithranol + CF_3CO_2Ag) m/z calcd for $C_{22}H_{36}BrI$ + Ag^+ $[M + Ag]^+$ 613.0091, found 613.0078; Anal. Calcd for $C_{22}H_{36}BrI$: C, 52.08; H, 7.15. Found: C, 52.27; H, 7.29.

[(3-Bromo-5-hexadecylphenyl)ethynyl]triisopropylsilane (10) from 16. To a degassed solution of **16** (3.04 g, 5.99 mmol), CuI (120 mg, 0.629 mmol), $PdCl_2(PPh_3)_2$ (214 mg, 0.305 mmol), and triethylamine (45 mL) in THF (60 mL) was added a solution of TIPS acetylene (1.34 g, 7.33 mmol) in a small amount of THF. The resulting mixture was stirred at 50 °C for 4 h under an Ar atmosphere. The reaction mixture was poured into a 5% NH_4Cl solution and extracted with toluene. The organic layer was washed with a 5% NH_4Cl solution, dried over $MgSO_4$, and concentrated under reduced pressure. The residue was purified by column chromatography on silica gel with hexane and GPC with chloroform to afford **10** (3.24 g, 96%).

[(4′-Amino-5-hexadecylbiphenyl-3-yl)ethynyl]-triisopropylsilane (17). A solution of **10** (1.67 g, 2.97 mmol), 4-(4,4,5,5-tetramethyl-1,3,2-dioxaborolan-2-yl)aniline (790 mg, 3.61 mmol), 2 M Na_2CO_3 solution (6 mL), and $Pd(PPh_3)_4$ (87.2 mg, 75.5 mmol) in toluene (25 mL) was stirred at 120 °C for 24 h under an Ar atmosphere. The reaction mixture was poured into water and extracted with dichloromethane. The organic layer was washed with water, dried over $MgSO_4$, and concentrated under reduced pressure. The residue was purified by column chromatography on silica gel with dichloromethane/hexane (1:1) to afford **17** (1.52 g, 89%). Yellow oil; IR (neat): $\tilde{\nu}$ = 3475 (w, NH_2), 3384 (m, NH_2), 3219 (w, NH_2), 3027 (w), 2924 (s), 2853 (s), 2151 (m, C≡C), 1622 (s), 1591 (s), 1519 (s), 1464 (s), 1401 (w), 1382 (w), 1360 (w), 1285 (m), 1206 (w), 1183 (m), 1158 (w), 1127 (w), 1073 (w), 1018 (m), 996 (m), 968 (w), 919 (w), 882 (s), 826 (s), 719 (m), 690 (s), 674 (s), 614 (w), 579 (w), 554 (m), 511 (m), 500 (m), 464 (m), 420 (w) cm^{-1}; UV/vis (CH_2Cl_2): λ (log ε) = 227 (4.26), 243 sh (4.25), 257 (4.52), 267 (4.60), 284 (4.30) nm; ^1H NMR (500 MHz, $CDCl_3$, rt): δ = 7.45 (dd, J = 1.7, 1.5 Hz, 1H, 2-H), 7.39 (d, J = 8.5 Hz, 2H, 2′,6′-H), 7.28 (br. dd, J = 1.7, 1.6 Hz, 1H, 6-H), 7.20 (br. dd, 1H, 4-H), 6.75 (d, J = 8.5 Hz, 2H, 3′,5′-H), 3.73 (br. s, 2H, 4′-NH_2), 2.60 (t, J = 7.7 Hz, 2H, 1‴-H), 1.63 (tt, J = 7.7, 7.1 Hz, 2H, 2‴-H), 1.37−1.25 (m, 26H, 3‴-15‴-H), 1.14 (s, 21H, TIPS), 0.88 (t, J = 6.9 Hz, 3H, 16‴-H); ^{13}C NMR (125 MHz, $CDCl_3$, rt): δ = 145.84 (C-1 or C-4′), 143.32 (C-5), 141.12 (C-1 or C-4′), 131.01 (C-1′), 129.87 (C-4), 128.03 (C-2′,6′), 127.48 (C-2), 126.85 (C-6), 123.57 (C-3), 115.36 (C-3′,5′), 107.63 (C-1″), 89.63 (C-2″), 35.87 (C-1‴), 31.92 (C-14‴), 31.46 (C-2‴), 29.69 (t, 3C), 29.68 (t), 29.67 (t, 2C), 29.65 (t), 29.59 (t), 29.50 (t), 29.37 (t), 29.35 (t), 22.68 (C-15‴), 18.69 (q, TIPS), 14.11 (C-16‴), 11.34 (d, TIPS); HR-MALDI-MS (dithranol + CF_3CO_2Ag) m/z calcd for $C_{39}H_{63}NSi$ + Ag^+ $[M + Ag]^+$ 680.3775, found 680.3785; HR-MALDI-MS (dithranol + CF_3CO_2Na) m/z calcd for $C_{39}H_{63}NSi$ + Na^+ $[M + Na]^+$ 596.4622, found 596.4684.

{[4′-(3,3-Diethyl-2-triazeno)-5-hexadecylbiphenyl-3-yl]-ethynyl}triisopropylsilane (18). To a solution of **17** (1.98 g, 3.45 mmol) in dry dichloromethane (34 mL) were added dropwise a solution of boron trifluoride−diethyl ether complex (1.1 mL, 8.7 mmol) in dichloromethane (3 mL) and a solution of isoamyl nitrite (1.2 mL, 9.0 mmol) in dichloromethane (3 mL) at −15 °C under an Ar atmosphere. The mixture was stirred at the same temperature for 30 min. After warming the reaction mixture to 0 °C, diethylamine (3.6 mL, 35 mmol) and potassium carbonate (4.06 g, 29.4 mmol) were added to the mixture, and the mixture was stirred at the same temperature for 2 h. The reaction mixture was poured into water and extracted with dichloromethane. The organic layer was washed with water, dried over $MgSO_4$, and concentrated under reduced pressure. The residue was purified by column chromatography on Al_2O_3 with dichloromethane/hexane (1:9) to afford **18** (1.99 g, 88%). Yellow oil; IR (neat): $\tilde{\nu}$ = 3031 (w), 2925 (s), 2854 (s), 2151 (m, C≡C), 1591 (m), 1504 (m), 1464 (s), 1414 (s), 1383 (s), 1342 (s), 1235 (s), 1200 (m), 1164 (m), 1098 (s), 1069 (m), 1011 (w), 996 (m), 969 (w), 919 (w), 883 (s), 853 (w), 838 (s), 805 (w), 763 (w), 715 (w), 695 (s), 676 (s), 660 (m), 612 (w), 567 (w), 533 (w), 500 (w), 464 (w) cm^{-1}; UV/vis (CH_2Cl_2): λ (log ε) = 241 (4.37), 251 (4.37), 270 (4.33), 300 sh (4.27), 334 (4.41) nm; ^1H NMR (500 MHz, $CDCl_3$, rt): δ = 7.55 (d, J = 8.6 Hz, 2H, 2′,6′-H or 3′,5′-H), 7.52 (dd, J = 1.6, 1.4 Hz, 1H, 2-H), 7.47 (d, J = 8.6 Hz, 2H, 2′,6′-H or 3′,5′-H), 7.35 (br. dd, J = 1.6, 1.6 Hz, 1H, 6-H), 7.24 (br. dd, 1H, 4-H), 3.78 (q, J = 7.2 Hz, 4H, 4′-N_3Et_2), 2.62 (t, J = 7.8 Hz, 2H, 1‴-H), 1.64 (tt, J = 7.8, 7.1 Hz, 2H, 2‴-H), 1.37−1.25 (m, 26H, 3‴-15‴-H), 1.28 (t, J = 7.2 Hz, 6H, 4′-N_3Et_2), 1.15 (s, 21H, TIPS), 0.88 (t, J = 7.0 Hz, 3H, 16‴-H); ^{13}C NMR (125 MHz, $CDCl_3$, rt): δ = 150.69 (C-1 or C-4′), 143.38 (C-5), 141.08 (C-1 or C-4′), 137.14 (C-1′), 130.43 (C-4), 127.88 (C-2), 127.51 (C-2′,6′ or C-3′,5′), 127.25 (C-6), 123.65 (C-3), 120.71 (C-2′,6′ or C-3′,5′), 107.52 (C-1″), 89.83 (C-2″), 35.87 (C-1‴), 31.92 (C-14‴), 31.47 (C-2‴), 29.69 (t, 3C), 29.68 (t), 29.67 (t, 2C), 29.65 (t), 29.60 (t), 29.50 (t), 29.38 (t), 29.36 (t), 22.68 (C-15‴), 18.70 (q, TIPS), 14.11 (C-16‴), 11.34 (d, TIPS); HR-MALDI-MS (dithranol + CF_3CO_2Ag) m/z calcd for $C_{43}H_{71}N_3Si$ + Ag^+ $[M + Ag]^+$ 764.4463, found 764.4463; HR-MALDI-MS (dithranol + CF_3CO_2Na) m/z calcd for $C_{43}H_{71}N_3Si$ + Na^+ $[M + Na]^+$ 680.5309, found 680.5303; HR-MALDI-MS (dithranol) m/z calcd for $C_{43}H_{71}N_3Si$ + H^+ $[M + H]^+$ 658.5490, found: 658.5481.

[(5-Hexadecyl-4′-iodobiphenyl-3-yl)ethynyl]-triisopropylsilane (19). A solution of **18** (1.42 g, 2.16 mmol) in iodomethane (15 mL) was stirred at 120 °C for 24 h in an autoclave. The reaction mixture was poured into a 10% $NaHSO_3$ solution and extracted with dichloromethane. The organic layer was washed with a 10% $NaHSO_3$ solution, dried over $MgSO_4$, and concentrated under reduced pressure. The residue was purified by column chromatography on silica gel with dichloromethane/hexane (1:4) to afford **19** (1.44 g, 97%). Yellow crystals; mp 43.8−45.0 °C (methanol); IR (KBr disk): $\tilde{\nu}$ = 3042 (w), 2916 (s), 2851 (s), 2151 (m, C≡C), 1593 (m), 1486 (m), 1471 (s), 1382 (m), 1363 (w), 1249 (w), 1234 (w), 1202 (w), 1181 (w), 1164 (w), 1074 (m), 1053 (w), 1011 (w), 1005 (m), 959 (w), 913 (w), 882 (m), 853 (m), 820 (m), 707 (m), 690 (m), 671 (m), 659 (m), 632 (w), 564 (w), 494 (w) cm^{-1}; UV/vis (CH_2Cl_2): λ (log ε) = 242 sh (4.42), 255 (4.66), 265 (4.62), 286 sh (4.07) nm; ^1H NMR (500 MHz, $CDCl_3$, rt): δ = 7.75 (d, J = 8.5 Hz, 2H, 2′,6′-H or 3′,5′-H), 7.46 (dd, J = 1.5, 1.5 Hz, 1H, 2-H), 7.31 (d, J = 8.5 Hz, 2H, 2′,6′-H or 3′,5′-H), 7.28 (d, J = 1.5 Hz, 2H, 4-H and 6-H), 2.62 (t, J = 7.8 Hz, 2H, 1‴-H), 1.63 (tt, J = 7.8, 7.1 Hz, 2H, 2‴-H), 1.38−1.25 (m, 26H, 3‴-15‴-H), 1.14 (s, 21H, TIPS), 0.88 (t, J = 7.0 Hz, 3H, 16‴-H); ^{13}C NMR (125 MHz, $CDCl_3$, rt): δ = 143.71 (C-5), 140.15 (C-1 or C-1′), 140.10 (C-1 or C-1′), 137.80 (C-2′,6′ or C-3′,5′), 131.23 (C-4 or C-6), 129.01 (C-2′,6′ or C-3′,5′), 127.90 (C-2), 127.20 (C-4 or C-6), 123.95 (C-3), 107.06 (C-1″), 93.21 (C-4′), 90.41 (C-2″), 35.81 (C-1‴), 31.93 (C-14‴), 31.44 (C-2‴), 29.70 (t, 3C), 29.69 (t), 29.66 (t, 3C), 29.58 (t), 29.48 (t), 29.37 (t), 29.34 (t), 22.69 (C-15‴), 18.69 (q, TIPS), 14.13 (C-16‴), 11.32 (d, TIPS); HR-MALDI-MS (dithranol + CF_3CO_2Ag) m/z calcd for $C_{39}H_{61}ISi$ + Ag^+ $[M + Ag]^+$ 791.2633, found 791.2636; Anal. Calcd for $C_{39}H_{61}ISi$: C, 68.39; H, 8.98. Found: C, 68.70; H, 8.97.

(3′-Ethynyl-5′-hexadecylbiphenyl-4-yl)-3,3-diethyltriazene (20). A solution of TBAF (1.0 mol/L, 3.2 mL, 3.2 mmol) in THF was added to a solution of **18** (1.04 g, 1.58 mmol) in THF (10 mL). After stirring the mixture at room temperature for 4 h, the reaction mixture was poured into water and extracted with dichloromethane. The organic layer was washed with brine, dried over $MgSO_4$, and concentrated under reduced pressure. The residue was purified by column chromatography on Al_2O_3 with dichloromethane/hexane (1:1) and GPC with chloroform to afford **20** (772 mg, 97%). Pale

DOI: 10.1021/acs.joc.5b00485
J. Org. Chem. 2015, 80, 5092−5110

yellow crystals; mp 54.4−55.0 °C (EtOH); IR (KBr disk): $\tilde{\nu}$ = 3291 (m, C≡C−H), 3258 (m), 3032 (w), 2920 (s), 2848 (s), 2106 (w, C≡C), 1591 (m), 1503 (m), 1464 (s), 1439 (s), 1418 (s), 1392 (s), 1339 (s), 1238 (s), 1204 (m), 1166 (m), 1102 (s), 998 (w), 950 (w), 877 (m), 841 (s), 804 (m), 762 (w), 724 (m), 692 (m), 653 (m), 606 (m), 569 (m), 557 (m), 536 (w), 473 (w) cm^{-1}; UV/vis (CH_2Cl_2): λ (log ε) = 234 (4.39), 258 sh (3.93), 296 sh (4.19), 335 (4.38) nm; ^{1}H NMR (500 MHz, $CDCl_3$, rt): δ = 7.56 (br. dd, J = 1.5, 1.5 Hz, 1H, 2′-H), 7.55 (d, J = 8.6 Hz, 2H, 2,6-H or 3,5-H), 7.48 (d, J = 8.6 Hz, 2H, 2,6-H or 3,5-H), 7.40 (br. dd, 1H, 6′-H), 7.27 (br. dd, 1H, 4′-H), 3.78 (q, J = 7.2 Hz, 4H, 4-N_3Et_2), 3.07 (s, 1H, 2″-H), 2.63 (t, J = 7.8 Hz, 2H, 1‴-H), 1.64 (tt, J = 7.8, 7.1 Hz, 2H, 2‴-H), 1.38−1.25 (m, 26H, 3‴-15‴-H), 1.28 (t, J = 7.2 Hz, 6H, 4-N_3Et_2), 0.88 (t, J = 6.9 Hz, 3H, 16‴-H); ^{13}C NMR (125 MHz, $CDCl_3$, rt): δ = 150.74 (C-4 or C-1′), 143.51 (C-5′), 141.16 (C-4 or C-1′), 136.87 (C-1), 130.48 (C-4′), 127.93 (C-2′), 127.70 (C-6′), 127.46 (C-2,6 or C-3,5), 122.16 (C-3′), 120.75 (C-2,6 or C-3,5), 84.05 (C-1″), 76.61 (C-2″), 35.81 (C-1‴), 31.91 (C-14‴), 31.36 (C-2‴), 29.69 (t, 3C), 29.68 (t), 29.66 (t, 2C), 29.65 (t), 29.56 (t), 29.48 (t), 29.35 (t), 29.29 (t), 22.68 (C-15‴), 14.11 (C-16‴); HR-MALDI-MS (dithranol + CF_3CO_2Ag) m/z calcd for $C_{34}H_{51}N_3$ − $N_3Et_2^+$ + $2Ag^+$ [M − N_3Et_2 + 2Ag]$^+$ 615.1305, found 615.1305; HR-MALDI-MS (dithranol + CF_3CO_2Na) m/z calcd for $C_{34}H_{51}N_3$ − $N_3Et_2^+$ + $2Na^+$ [M − N_3Et_2 + 2Na]$^+$ 447.2998, found 447.3016; HR-MALDI-MS (dithranol) m/z calcd for $C_{34}H_{51}N_3$ + H^+ [M + H]$^+$ 502.4156, found 502.4158; Anal. Calcd for $C_{34}H_{51}N_3$: C, 81.38; H, 10.24; N, 8.37. Found: C, 81.58; H, 10.53; N, 8.29.

{{4′-{[4′-(3,3-Diethyl-2-triazeno)-5-hexadecylbiphenyl-3-yl]-ethynyl}-5-hexadecylbiphenyl-3-yl}ethynyl}triisopropylsilane (21). To a degassed solution of **19** (1.27 g, 1.85 mmol), CuI (38.1 mg, 0.200 mmol), $Pd(PPh_3)_4$ (10.5 mg, 91.0 μmol), and triethylamine (15 mL) in THF (25 mL) was added dropwise at 85 °C for 3 h a solution of **20** (938 mg, 1.87 mmol) in THF (10 mL) divided into five portions. The resulting mixture was stirred at the same temperature for another 1 h under an Ar atmosphere. The reaction mixture was poured into a 5% NH_4Cl solution and extracted with dichloromethane. The organic layer was washed with a 5% NH_4Cl solution, dried over $MgSO_4$, and concentrated under reduced pressure. The residue was purified by column chromatography on Al_2O_3 with dichloromethane/hexane (1:1) and GPC with chloroform to afford **21** (1.87 g, 95%). Yellowish brown oil; IR (neat): $\tilde{\nu}$ = 3035 (w), 2924 (s), 2853 (s), 2152 (m, C≡C), 1591 (s), 1511 (m), 1465 (s), 1418 (m), 1393 (m), 1378 (s), 1338 (s), 1330 (s), 1235 (s), 1204 (m), 1164 (m), 1098 (s), 1075 (m), 1017 (m), 996 (m), 931 (w), 882 (s), 836 (s), 807 (w), 765 (w), 722 (w), 687 (s), 609 (w), 578 (w), 545 (w), 500 (w), 464 (w) cm^{-1}; UV/vis (CH_2Cl_2): λ (log ε) = 228 (4.50), 232 sh (4.49), 245 sh (4.42), 255 (4.43), 269 (4.53), 312 (4.73), 328 sh (4.70) nm; ^{1}H NMR (500 MHz, $CDCl_3$, rt): δ = 7.63 (dd, J = 1.4, 1.4 Hz, 1H, 2‴″-H), 7.61 (d, J = 8.6 Hz, 2H, 2′,6′-H or 3′,5′-H), 7.59 (d, J = 8.5 Hz, 2H, 2‴″,6‴″-H or 3‴″, 5‴″-H), 7.58 (d, J = 8.6 Hz, 2H, 2′,6′-H or 3′,5′-H), 7.53 (dd, J = 1.5, 1.4 Hz, 1H, 2-H), 7.49 (d, J = 8.5 Hz, 2H, 2‴″,6‴″-H or 3‴″,5‴″-H), 7.39 (br. dd, 1H, 6‴″-H), 7.36 (br. dd, 1H, 6-H), 7.34 (br. dd, 1H, 4‴″-H), 7.29 (br. dd, 1H, 4-H), 3.79 (q, J = 7.2 Hz, 4H, 4‴″-N_3Et_2), 2.67 (t, J = 7.7 Hz, 2H, 1‴-H or 1‴″-H), 2.64 (t, J = 7.9 Hz, 2H, 1‴-H or 1‴″-H), 1.68 (tt, J = 7.7, 6.7 Hz, 2H, 2‴-H or 2‴″-H), 1.65 (tt, J = 7.9, 6.9 Hz, 2H, 2‴-H or 2‴″-H), 1.39−1.25 (m, 52H, 3‴-15‴-H or 3‴″-15‴″-H), 1.29 (t, J = 7.2 Hz, 6H, 4‴″-N_3Et_2), 1.15 (s, 21H, TIPS), 0.88 (t, J = 6.9 Hz, 6H, 16‴-H or 16‴″-H); ^{13}C NMR (125 MHz, $CDCl_3$, rt): δ = 150.72 (C-4‴″), 143.64 (C-5 or C-5‴″), 143.54 (C-5 or C-5‴″), 141.19 (s), 140.44 (s), 140.27 (s), 137.08 (s), 132.02 (C-2′,6′ or C-3′,5′), 131.16 (C-4), 130.01 (C-4‴″), 128.03 (C-2), 127.50 (C-2‴″,6‴″ or C-3‴″,5‴″), 127.43 (C-2‴″), 127.35 (C-6), 127.26 (C-6‴″), 127.03 (C-2′,6′ or C-3′,5′), 123.89 (s), 123.34 (s), 122.51 (s), 120.76 (C-2‴″,6‴″ or C-3‴″,5‴″), 107.19 (C-1″), 90.61 (C-2″ or C-2‴″), 90.25 (C-2″ or C-2‴″), 88.84 (C-1‴″), 35.91 (t), 35.85 (t), 31.92 (t), 31.47 (t), 31.43 (t), 29.70 (t), 29.68 (t), 29.67 (t), 29.66 (t), 29.59 (t), 29.52 (t), 29.49 (t), 29.37 (t), 29.36 (t), 29.35 (t), 22.69 (t), 18.70 (q, TIPS), 14.12 (q), 11.34 (d, TIPS); HR-MALDI-MS (dithranol) m/z calcd for $C_{73}H_{111}N_3Si$ + H^+ [M + H]$^+$ 1058.8620, found 1058.8630.

{{4′-[(4′-Iodo-5-hexadecylbiphenyl-3-yl)ethynyl]-5-hexadecylbiphenyl-3-yl]ethynyl}triisopropylsilane (4). A solution of **21** (560 mg, 0.529 mmol) in iodomethane (15 mL) was stirred at 120 °C for 1.5 days in an autoclave. The reaction mixture was poured into a 10% $NaHSO_3$ solution and extracted with dichloromethane. The organic layer was washed with a 10% $NaHSO_3$ solution, dried over $MgSO_4$, and concentrated under reduced pressure. The residue was purified by column chromatography on silica gel with dichloromethane/hexane (1:4) to afford **4** (562 mg, 98%). Yellow oil; IR (neat): $\tilde{\nu}$ = 3037 (w), 2923 (s), 2853 (s), 2153 (m, C≡C), 1591 (s), 1565 (w), 1512 (m), 1490 (m), 1465 (s), 1382 (m), 1373 (w), 1308 (w), 1243 (w), 1108 (w), 1072 (w), 1015 (w), 1005 (m), 992 (m), 968 (w), 920 (w), 882 (s), 833 (s), 819 (m), 759 (w), 721 (w), 689 (m), 670 (m), 610 (w), 578 (w), 551 (w), 529 (w), 500 (w), 464 (w) cm^{-1}; UV/vis (CH_2Cl_2): λ (log ε) = 246 sh (4.45), 256 sh (4.52), 269 (4.64), 291 sh (4.54), 306 (4.57), 324 sh (4.46) nm; ^{1}H NMR (500 MHz, $CDCl_3$, rt): δ = 7.77 (d, J = 8.5 Hz, 2H, 2‴″,6‴″-H or 3‴″,5‴″-H), 7.61 (d, J = 8.6 Hz, 2H, 2′,6′-H or 3′,5′-H), 7.58 (d, J = 8.6 Hz, 2H, 2′,6′-H or 3′,5′-H), 7.56 (dd, J = 1.6, 1.5 Hz, 1H, 2‴″-H), 7.53 (dd, J = 1.5, 1.5 Hz, 1H, 2-H), 7.38 (br. dd, 1H, 4‴″-H), 7.36 (br. dd, 1H, 6-H), 7.35 (d, J = 8.5 Hz, 2H, 2‴″,6‴″-H or 3‴″,5‴″-H), 7.33 (br. dd, 1H, 6‴″-H), 7.29 (br. dd, 1H, 4-H), 2.67 (t, J = 7.7 Hz, 2H, 1‴-H or 1‴″-H), 2.64 (t, J = 8.0 Hz, 2H, 1‴-H or 1‴″-H), 1.67 (tt, J = 7.7, 7.5 Hz, 2H, 2‴-H or 2‴″-H), 1.65 (tt, J = 8.1, 8.0 Hz, 2H, 2‴-H or 2‴″-H), 1.39−1.25 (m, 52H, 3‴-15‴-H and 3‴″-15‴″-H), 1.15 (s, 21H, TIPS), 0.88 (t, J = 6.9 Hz, 6H, 16‴-H and 16‴″-H); ^{13}C NMR (125 MHz, $CDCl_3$, rt): δ = 143.84 (C-5 or C-5‴″), 143.65 (C-5 or C-5‴″), 140.42 (s), 140.36 (s), 140.18 (s), 140.08 (s), 137.84 (C-2‴″,6‴″ or C-3‴″,5‴″), 132.01 (C-2′,6′ or C-3′,5′), 131.21 (C-4), 130.81 (C-4‴″), 128.98 (C-2‴″,6‴″ or C-3‴″,5‴″), 128.02 (C-2), 127.45 (C-2‴″), 127.34 (C-6), 127.19 (C-6‴″), 127.07 (C-2′,6′ or C-3′,5′), 123.90 (s), 123.66 (s), 122.28 (s), 107.15 (C-1″), 93.28 (C-4‴″), 90.29 (C-2″ or C-2‴″), 90.17 (C-2″ or C-2‴″), 89.24 (C-1‴″), 35.84 (t), 31.92 (t), 31.47 (t), 31.38 (t), 29.70 (t), 29.67 (t), 29.65 (t), 29.59 (t), 29.57 (t), 29.49 (t), 29.36 (t), 29.30 (t), 22.69 (t), 18.70 (q, TIPS), 14.12 (q), 11.33 (d, TIPS); HR-MALDI-MS (dithranol + CF_3CO_2Ag) m/z calcd for $C_{69}H_{101}ISi$ + Ag^+ [M + Ag]$^+$ 1191.5763, found 1191.5797.

{3′-[(3′-Ethynyl-5′-hexadecylbiphenyl-4-yl)ethynyl]-5′-hexadecylbiphenyl-4-yl}-3,3-diethyltriazene (5). A solution of TBAF (1.0 mol/L, 2.4 mL, 2.4 mmol) in THF was added to a solution of **21** (1.24 g, 1.17 mmol) in THF (10 mL). After stirring the mixture at room temperature for 1 h, the reaction mixture was poured into water and extracted with dichloromethane. The organic layer was washed with water, dried over $MgSO_4$, and concentrated under reduced pressure. The residue was purified by column chromatography on Al_2O_3 with dichloromethane and GPC with chloroform to afford **5** (972 mg, 92%). Yellowish brown crystals; mp 33.9−34.8 °C (acetone); IR (neat): $\tilde{\nu}$ = 3284 (m, C≡C−H), 3035 (w), 2919 (s), 2850 (s), 1591 (s), 1511 (m), 1465 (s), 1448 (s), 1415 (m), 1393 (m), 1341 (m), 1236 (s), 1204 (m), 1165 (m), 1099 (s), 1018 (w), 1000 (w), 949 (w), 879 (m), 837 (s), 799 (w), 765 (w), 721 (m), 698 (m), 644 (w), 605 (w), 571 (w), 534 (w) cm^{-1}; UV/vis (CH_2Cl_2): λ (log ε) = 230 (4.57), 242 sh (4.46), 256 sh (4.29), 312 (4.76), 327 sh (4.73) nm; ^{1}H NMR (500 MHz, $CDCl_3$, rt): δ = 7.624 (br. dd, 1H, 2′-H), 7.617 (d, J = 8.5 Hz, 2H, 2‴″,6‴″-H or 3‴″,5‴″-H), 7.59 (d, J = 8.7 Hz, 2H, 2,6-H or 3,5-H), 7.570 (d, J = 8.5 Hz, 2H, 2‴″,6‴″-H or 3‴″,5‴″-H), 7.567 (dd, J = 1.7, 1.7 Hz, 1H, 2‴″-H), 7.49 (d, J = 8.7 Hz, 2H, 2,6-H or 3,5-H), 7.401 (br. dd, 1H, 6‴″-H), 7.395 (br. dd, 1H, 6′-H), 7.33 (br. dd, 1H, 4′-H), 7.31 (br. dd, 1H, 4‴″-H), 3.79 (q, J = 7.2 Hz, 4H, 4-N_3Et_2), 3.08 (s, 1H, 2‴″-H), 2.66 (t, J = 7.6 Hz, 2H, 1‴-H or 1‴″-H), 2.64 (t, J = 7.3 Hz, 2H, 1‴-H or 1‴″-H), 1.68 (tt, J = 7.6, 7.1 Hz, 2H, 2‴-H or 1‴″-H), 1.65 (tt, J = 7.6, 7.1 Hz, 2H, 2‴-H or 2‴″-H), 1.40−1.25 (m, 52H, 3‴-15‴-H and 3‴″-15‴″-H), 1.29 (t, J = 7.2 Hz, 6H, 4-N_3Et_2), 0.88 (t, J = 6.8 Hz, 6H, 16‴-H and 16‴″-H); ^{13}C NMR (125 MHz, $CDCl_3$, rt): δ = 150.71 (C-4), 143.75 (C-5′ or C-5‴″), 143.53 (C-5′ or C-5‴″), 141.18 (s), 140.51 (s), 140.01 (s), 137.05 (s), 132.05 (C-2‴″,6‴″ or C-3‴″,5‴″), 131.21 (C-4‴″), 130.00 (C-4′), 128.12 (C-2‴″),

DOI: 10.1021/acs.joc.5b00485
J. Org. Chem. 2015, 80, 5092−5110

127.81 (C-6′), 127.49 (C-2,6 or C-3,5), 127.42 (C-2′), 127.27 (C-6′), 126.98 (C-2′′′′,6′′′′ or C-3′′′′,5′′′′), 123.30 (s), 122.62 (s), 122.43 (s), 120.75 (C-2,6 or C-3,5), 90.70 (C-1′′), 88.76 (C-2′′), 83.77 (C-1′′′′′′), 76.94 (C-2′′′′′′), 35.90 (t), 35.79 (t), 31.92 (t), 31.42 (t), 31.35 (t), 29.69 (t), 29.68 (t), 29.65 (t), 29.59 (t), 29.56 (t), 29.52 (t), 29.48 (t), 29.36 (t), 29.34 (t), 29.28 (t), 22.68 (t), 14.12 (q); HR-MALDI-MS (dithranol) m/z calcd for $C_{64}H_{91}N_3$ + H^+ $[M + H]^+$ 902.7286, found 902.7328; Anal. Calcd for $C_{64}H_{91}N_3$: C, 85.18; H, 10.16; N, 4.66. Found: C, 85.06; H, 10.22; N, 4.61.

{{4′-{{4′-{{4′-{[4′-(3,3-Diethyl-2-triazeno)-5-hexadecylbiphenyl-3-yl]ethynyl}-5-hexadecylbiphenyl-3-yl}ethynyl}-5-hexadecylbiphenyl-3-yl}ethynyl}-5-hexadecylbiphenyl-3-yl}ethynyl}triisopropylsilane (22). To a degassed solution of **4** (562 mg, 0.518 mmol), CuI (13.7 mg, 71.9 μmol), $Pd(PPh_3)_4$ (33.4 mg, 28.9 μmol), and triethylamine (10 mL) in THF (20 mL) was added dropwise at 90 °C for 3 h a solution of **5** (473 mg, 0.524 mmol) in THF (10 mL) divided into four potions. The resulting mixture was stirred at the same temperature for another 2 h under an Ar atmosphere. The reaction mixture was poured into a 5% NH_4Cl solution and extracted with dichloromethane. The organic layer was washed with a 5% NH_4Cl solution, dried over $MgSO_4$, and concentrated under reduced pressure. The residue was purified by column chromatography on Al_2O_3 with dichloromethane/hexane (1:1) and GPC with chloroform to afford **22** (844 mg, 88%). Yellowish brown oil; IR (neat): $\tilde{\nu}$ = 3035 (m), 2923 (s), 2851 (s), 2152 (m, C≡C), 1590 (s), 1554 (w), 1512 (s), 1465 (s), 1419 (m), 1393 (m), 1381 (m), 1352 (m), 1235 (m), 1204 (m), 1164 (m), 1097 (m), 1079 (m), 1018 (m), 995 (m), 970 (w), 960 (w), 934 (w), 881 (s), 834 (s), 790 (w), 764 (w), 760 (w), 725 (m), 698 (m), 681 (m), 608 (m), 575 (w), 570 (w), 536 (w), 500 (w), 464 (w) cm^{-1}; UV/vis (CH_2Cl_2): λ (log ε) = 229 (4.70), 232 sh (4.67), 244 sh (4.51), 256 (4.50), 270 (4.64), 314 (5.05), 327 sh (5.03), 362 sh (4.05) nm; ^{1}H NMR (500 MHz, $CDCl_3$, rt): δ = 7.65−7.58 (m, 17H), 7.53 (dd, J = 1.4, 1.4 Hz, 1H, 2-H), 7.50 (d, J = 8.6 Hz, 2H, 2′′′′′′,6′′′′′′-H or 3′′′′′′,5′′′′′′-H), 7.40−7.39 (m, 5H), 7.36 (br. dd, 1H, 6-H), 7.34 (br. dd, 1H, 4′′′′′-H), 7.29 (br. dd, 1H, 4-H), 3.79 (q, J = 7.2 Hz, 4H, 4′′′′′′-N_3Et_2), 2.70−2.62 (m, 8H), 1.72−1.62 (m, 8H), 1.41−1.26 (m, 104H), 1.29 (t, J = 7.2 Hz, 6H, 4′′′′′′-N_3Et_2), 1.15 (s, 21H, TIPS), 0.87 (t, J = 6.9 Hz, 12H); ^{13}C NMR (125 MHz, $CDCl_3$): δ = 150.72 (C-4′′′′′′), 143.79 (s), 143.78 (s), 143.65 (s), 143.53 (s), 141.19 (s), 140.54 (s), 140.49 (s), 140.39 (s), 140.32 (s), 140.21 (s), 137.07 (s), 132.06 (d), 132.02 (d), 131.20 (d), 130.75 (d), 130.73 (d), 130.01 (C-4′′′′′), 128.03 (C-2), 127.64 (d), 127.50 (C-2′′′′′′,6′′′′′′ or C-3′′′′′′,5′′′′′′), 127.43 (d), 127.34 (d), 127.26 (d), 127.06 (d), 127.04 (d), 127.02 (d), 123.90 (s), 123.62 (s), 123.60 (s), 123.34 (s), 122.56 (s), 122.42 (s), 122.36 (s), 120.76 (C-2′′′′′′,6′′′′′′ or C-3′′′′′′,5′′′′′′), 107.17 (C-1′′), 90.68 (s), 90.37 (s), 90.30 (s), 90.28 (s), 89.17 (s), 89.14 (s), 88.84 (s), 35.91 (t), 35.89 (t), 35.85 (t), 31.92 (t), 31.47 (t), 31.42 (t), 29.70 (t), 29.68 (t), 29.67 (t), 29.66 (t), 29.59 (t), 29.53 (t), 29.52 (t), 29.49 (t), 29.38 (t), 29.36 (t), 29.35 (t), 29.33 (t), 22.69 (t), 18.70 (q, TIPS), 14.12 (q), 11.33 (d, TIPS); HR-MALDI-MS (dithranol) m/z calcd for $C_{133}H_{191}N_3Si$ + H^+ $[M + H]^+$ 1859.4880, found 1859.4840.

{{4′-{{4′-{{4′-[(4′-Iodo-5-hexadecylbiphenyl-3-yl)ethynyl]-5-hexadecylbiphenyl-3-yl}ethynyl}-5-hexadecylbiphenyl-3-yl}ethynyl}-5-hexadecylbiphenyl-3-yl}ethynyl}triisopropylsilane (23). A solution of **22** (844 mg, 0.454 mmol) in iodomethane (17 mL) was stirred at 120 °C for 2 days in an autoclave. The reaction mixture was poured into a 10% $NaHSO_3$ solution and extracted with dichloromethane. The organic layer was washed with a 10% $NaHSO_3$ solution, dried over $MgSO_4$, and concentrated under reduced pressure. The residue was purified by column chromatography on silica gel with dichloromethane/hexane (1:4) to afford **23** (844 mg, 99%). Yellow oil; IR (neat): $\tilde{\nu}$ = 3036 (m), 2923 (s), 2852 (s), 2152 (m, C≡C), 1591 (s), 1553 (w), 1512 (s), 1492 (m), 1465 (s), 1402 (m), 1382 (m), 1374 (m), 1300 (w), 1244 (w), 1109 (w), 1072 (w), 1020 (m), 1006 (m), 1000 (m), 978 (w), 930 (w), 881 (s), 833 (s), 820 (s), 760 (w), 726 (m), 698 (s), 691 (s), 607 (w), 575 (w), 560 (w), 536 (w), 500 (w), 464 (w) cm^{-1}; UV/vis (CH_2Cl_2): λ (log ε) = 228 (4.84), 233 sh (4.79), 255 sh (4.61), 270 sh (4.76), 314 (5.20), 328 sh (5.18), 359 sh (4.16) nm; ^{1}H NMR (500 MHz, $CDCl_3$, rt): δ = 7.78 (d, J = 8.5 Hz, 2H, 2′′′′′′,6′′′′′′-H or 3′′′′′′,5′′′′′′-H), 7.64−7.58 (m, 14H), 7.57 (br. dd, 1H, 2′′′′′-H), 7.53 (br. dd, 1H, 2-H), 7.40−7.39 (m, 5H), 7.364 (br. dd, 1H, 6-H), 7.356 (d, J = 8.5 Hz, 2H, 2′′′′′′,6′′′′′′-H or 3′′′′′′,5′′′′′′-H), 7.33 (br. dd, 1H, 6′′′′′-H), 7.29 (br. dd, 1H, 4-H), 2.70−2.62 (m, 8H), 1.72−1.62 (m, 8H), 1.41−1.26 (m, 104H), 1.15 (s, 21H, TIPS), 0.87 (t, J = 6.6 Hz, 12H); ^{13}C NMR (125 MHz, $CDCl_3$, rt): δ = 143.85 (s), 143.80 (s), 143.65 (s), 140.48 (s), 140.47 (s), 140.39 (s), 140.38 (s), 140.37 (s), 140.34 (s), 140.19 (s), 140.09 (s), 137.85 (C-2′′′′′′,6′′′′′′ or C-3′′′′′′,5′′′′′′), 132.06 (d), 132.02 (d), 131.20 (C-4), 130.81 (d), 130.77 (d), 128.98 (C-2′′′′′′,6′′′′′′ or C-3′′′′′′,5′′′′′′), 128.03 (C-2), 127.63 (d), 127.45 (d), 127.34 (d), 127.20 (d), 127.07 (d), 127.05 (d), 123.90 (s), 123.67 (s), 123.62 (s), 122.38 (s), 122.34 (s), 107.16 (C-1′′), 93.28 (C-4′′′′′′), 90.33 (s), 90.28 (s), 90.23 (s), 89.23 (s), 89.17 (s), 35.89 (t), 35.85 (t), 31.92 (t), 31.47 (t), 31.42 (t), 31.38 (t), 29.79 (t), 29.78 (t), 29.70 (t), 29.68 (t), 29.66 (t), 29.59 (t), 29.57 (t), 29.51 (t), 29.49 (t), 29.37 (t), 29.36 (t), 29.33 (t), 29.30 (t), 22.69 (t), 18.70 (q, TIPS), 14.12 (q), 11.38 (d, TIPS); HR-MALDI-MS (dithranol + CF_3CO_2Ag) m/z calcd for $C_{129}H_{181}ISi$ + Ag^+ $[M + Ag]^+$ 1992.2023, found 1992.2029.

{{4′-{{4′-{{4′-{{4′-{{4′-{[4′-(3,3-Diethyl-2-triazeno)-5-hexadecylbiphenyl-3-yl]ethynyl}-5-hexadecylbiphenyl-3-yl}ethynyl}-5-hexadecylbiphenyl-3-yl}ethynyl}-5-hexadecylbiphenyl-3-yl}ethynyl}-5-hexadecylbiphenyl-3-yl}ethynyl}-5-hexadecylbiphenyl-3-yl}ethynyl}triisopropylsilane (24). To a degassed solution of **23** (531 mg, 0.281 mmol), CuI (6.4 mg, 34 mmol), $Pd(PPh_3)_4$ (18.3 mg, 15.8 μmol), and triethylamine (15 mL) in THF (25 mL) was added dropwise at 85 °C for 3.5 h a solution of **5** (255 mg, 0.283 mmol) in THF (10 mL) divided into four potions. The resulting mixture was stirred at the same temperature for another 1.5 h under an Ar atmosphere. The reaction mixture was poured into a 5% NH_4Cl solution and extracted with chloroform. The organic layer was washed with a 5% NH_4Cl solution, dried over $MgSO_4$, and concentrated under reduced pressure. The residue was purified by column chromatography on Al_2O_3 with dichloromethane/hexane (1:1) and GPC with chloroform to afford **24** (556 mg, 74%). Yellow oil; IR (neat): $\tilde{\nu}$ = 3035 (m), 2922 (s), 2851 (s), 2152 (m, C≡C), 1590 (s), 1552 (m), 1512 (s), 1465 (s), 1394 (m), 1379 (m), 1352 (m), 1235 (m), 1204 (m), 1164 (m), 1097 (m), 1081 (m), 1018 (m), 996 (m), 966 (w), 950 (w), 926 (w), 881 (s), 834 (s), 809 (m), 763 (w), 722 (m), 698 (m), 607 (m), 574 (m), 555 (w), 537 (m), 500 (w), 464 (w) cm^{-1}; UV/vis (CH_2Cl_2): λ (log ε) = 229 (4.93), 233 sh (4.88), 257 sh (4.70), 270 sh (4.85), 314 (5.29), 328 sh (5.27), 361 sh (4.05) nm; ^{1}H NMR (500 MHz, $CDCl_3$, rt): δ = 7.65−7.57 (m, 27H), 7.53 (br. dd, 1H, 2-H), 7.49 (d, J = 8.5 Hz, 2H, 2′′′′′′,6′′′′′′-H or 3′′′′′′,5′′′′′′-H), 7.41−7.39 (m, 9H), 7.36 (br. dd, 1H, 6-H), 7.34 (br. dd, 1H, 4′′′′′-H), 7.29 (br. dd, 1H, 4-H), 3.79 (q, J = 7.2 Hz, 4H, 4′′′′′′-N_3Et_2), 2.70−2.62 (m, 12H), 1.72−1.62 (m, 12H), 1.41−1.26 (m, 156H), 1.29 (t, J = 7.2 Hz, 6H, 4′′′′′′-N_3Et_2), 1.15 (s, 21H, TIPS), 0.87 (t, J = 6.9 Hz, 18H); ^{13}C NMR (125 MHz, $CDCl_3$, rt): δ = 150.72 (C-4′′′′′′), 143.80 (s), 143.78 (s), 143.65 (s), 143.54 (s), 141.20 (s), 140.55 (s), 140.51 (s), 140.50 (s), 140.40 (s), 140.35 (s), 140.33 (s), 140.22 (s), 137.08 (s), 132.07 (d), 132.02 (d), 131.20 (C-4), 130.77 (d), 130.73 (d), 130.01 (C-4′′′′′), 128.03 (C-2), 127.64 (d), 127.50 (C-2′′′′′′,6′′′′′′ or C-3′′′′′′,5′′′′′′), 127.44 (d), 127.34 (d), 127.27 (d), 127.07 (d), 127.05 (d), 127.02 (d), 123.91 (s), 123.63 (s), 123.61 (s), 123.35 (s), 122.57 (s), 122.43 (s), 122.42 (s), 122.36 (s), 120.76 (C-2′′′′′′,6′′′′′′ or C-3′′′′′′,5′′′′′′), 107.18 (C-1′′), 90.68 (s), 90.38 (s), 90.36 (s), 90.29 (s), 89.17 (s), 89.15 (s), 88.84 (s), 35.89 (t), 35.85 (t), 31.92 (t), 31.46 (t), 31.41 (t), 29.70 (t), 29.68 (t), 29.65 (t), 29.59 (t), 29.51 (t), 29.49 (t), 29.37 (t), 29.36 (t), 29.33 (t), 22.68 (t), 18.70 (q, TIPS), 14.11 (q), 11.34 (d, TIPS); HR-MALDI-MS (dithranol + CF_3CO_2Ag) m/z calcd for $C_{193}H_{271}N_3Si$ − $N_3Et_2^+$ + H^+ + Ag^+ $[M - N_3Et_2 + H + Ag]^+$ 2666.9316, found: 2666.9355.

{{4′-{{4′-{{4′-{{4′-{{4′-[(4′-Iodo-5-hexadecylbiphenyl-3-yl)ethynyl]-5-hexadecylbiphenyl-3-yl}ethynyl}-5-hexadecylbiphenyl-3-yl}ethynyl}-5-hexadecylbiphenyl-3-yl}ethynyl}-5-hexadecylbiphenyl-3-yl}ethynyl}-5-hexadecylbiphenyl-3-yl}ethynyl}triisopropylsilane (25). A solution of **24** (802 mg, 0.302 mmol) in iodomethane (16 mL) was stirred at 120 °C for 1.5 days in an autoclave. The reaction mixture was poured into a 10% $NaHSO_3$

DOI: 10.1021/acs.joc.5b00485
J. Org. Chem. 2015, 80, 5092−5110

solution and extracted with dichloromethane. The organic layer was dried over $MgSO_4$ and concentrated under reduced pressure. The residue was purified by column chromatography on silica gel with dichloromethane/hexane (1:3) to afford **25** (795 mg, 98%). Yellow oil; IR (neat): $\tilde{\nu}$ = 3035 (m), 2922 (s), 2851 (s), 2152 (w, C≡C), 1591 (s), 1553 (w), 1512 (s), 1495 (m), 1465 (s), 1396 (m), 1381 (m), 1300 (w), 1262 (w), 1109 (w), 1072 (w), 1020 (m), 1005 (m), 999 (m), 881 (s), 833 (s), 817 (s), 722 (m), 698 (s), 606 (w), 574 (w), 549 (w), 536 (w), 500 (w) cm^{-1}; UV/vis (CH_2Cl_2): λ (log ε) = 228 (4.84), 232 sh (4.81), 255 sh (4.74), 271 (4.88), 313 (5.19), 329 sh (5.14) nm; ^{1}H NMR (500 MHz, $CDCl_3$, rt): δ = 7.77 (d, J = 8.1 Hz, 2H, 2′′′′′′,6′′′′′′-H or 3′′′′′′,5′′′′′′-H), 7.65−7.57 (m, 24H), 7.57 (br. s, 1H, 2′′′′′-H), 7.53 (br. s, 1H, 2-H), 7.40−7.39 (m, 9H), 7.36 (br. s, 1H, 6-H), 7.35 (d, J = 8.1 Hz, 2H, 2′′′′′′,6′′′′′′-H or 3′′′′′′,5′′′′′′-H), 7.33 (br. s, 1H, 6′′′′′-H), 7.29 (br. s, 1H, 4-H), 2.70−2.62 (m, 12H), 1.72−1.62 (m, 12H), 1.41−1.26 (m, 156H), 1.15 (s, 21H, TIPS), 0.87 (t, J = 6.7 Hz, 18H); ^{13}C NMR (125 MHz, $CDCl_3$, rt): δ = 143.84 (s), 143.79 (s), 143.64 (s), 140.49 (s), 140.47 (s), 140.39 (s), 140.37 (s), 140.34 (s), 140.19 (s), 140.08 (s), 137.85 (C-2′′′′′′,6′′′′′′ or C-3′′′′′′,5′′′′′′), 132.07 (d), 132.02 (d), 131.21 (C-4), 130.81 (d), 130.77 (d), 128.97 (C-2′′′′′′,6′′′′′′ or C-3′′′′′′,5′′′′′′), 128.03 (C-2), 127.63 (d), 127.45 (d), 127.34 (d), 127.19 (d), 127.05 (d), 123.91 (s), 123.69 (s), 123.64 (s), 122.41 (s), 122.36 (s), 107.18 (C-1′′), 93.28 (C-4′′′′′′), 90.36 (s), 90.30 (s), 90.28 (s), 90.25 (s), 89.25 (s), 89.18 (s), 35.89 (t), 35.84 (t), 31.92 (t), 31.46 (t), 31.41 (t), 31.37 (t), 29.70 (t), 29.68 (t), 29.66 (t), 29.59 (t), 29.58 (t), 29.52 (t), 29.50 (t), 29.36 (t), 29.34 (t), 29.31 (t), 22.69 (t), 18.70 (q, TIPS), 14.12 (q), 11.34 (d, TIPS); HR-MALDI-MS (dithranol + CF_3CO_2Ag) m/z calcd for $C_{189}H_{261}ISi$ + Ag^+ $[M + Ag]^+$ 2792.8283, found 2792.8257.

3-Ethynyl-4′-{{4′-{{4′-{{4′-{{4′-{[(4′-iodo-5-hexadecylbiphenyl-3-yl)ethynyl]-5-hexadecylbiphenyl-3-yl}ethynyl}-5-hexadecylbiphenyl-3-yl}ethynyl}-5-hexadecylbiphenyl-3-yl}ethynyl}-5-hexadecylbiphenyl-3-yl}ethynyl}-5-hexadecylbiphenyl (26). A solution of TBAF (1.0 mol/L, 0.60 mL, 0.60 mmol) in THF was added to a solution of **25** (795 mg, 0.296 mmol) in THF (10 mL). After stirring the mixture at room temperature for 1.5 h, the reaction mixture was poured into water and extracted with dichloromethane. The organic layer was washed with water, dried over $MgSO_4$, and concentrated under reduced pressure. The residue was purified by column chromatography on silica gel with dichloromethane/hexane (1:4) and GPC with chloroform to afford **26** (736 mg, 98%). Yellow oil; IR (neat): $\tilde{\nu}$ = 3310 (w, C≡C−H), 3036 (m), 2922 (s), 2851 (s), 1590 (s), 1552 (w), 1512 (s), 1492 (m), 1465 (s), 1394 (m), 1378 (m), 1300 (w), 1272 (w), 1184 (w), 1109 (m), 1062 (w), 1018 (m), 1005 (m), 963 (w), 879 (s), 833 (s), 821 (s), 721 (s), 698 (s), 648 (m), 605 (m), 572 (w), 559 (w), 536 (w) cm^{-1}; UV/vis (CH_2Cl_2): λ (log ε) = 229 (4.94), 233 sh (4.89), 259 sh (4.76), 313 (5.29), 327 sh (5.25) nm; ^{1}H NMR (500 MHz, $CDCl_3$, rt): δ = 7.77 (d, J = 8.5 Hz, 2H, 2′′′′′′,6′′′′′′-H or 3′′′′′′,5′′′′′′-H), 7.65−7.57 (m, 10H), 7.57 (br. s, 2H, 2-H and 2′′′′′-H), 7.40−7.39 (m, 10H), 7.35 (d, J = 8.5 Hz, 2H, 2′′′′′′,6′′′′′′-H or 3′′′′′′,5′′′′′′-H), 7.33 (br. s, 1H, 6′′′′′-H), 7.32 (br. s, 1H, 4-H), 3.09 (s, 1H, 2″-H), 2.70−2.63 (m, 12H), 1.72−1.62 (m, 12H), 1.41−1.26 (m, 156H), 0.87 (t, J = 6.8 Hz, 18H); ^{13}C NMR (125 MHz, $CDCl_3$, rt): δ = 143.84 (s), 143.79 (s), 143.77 (s), 140.49 (s), 140.47 (s), 140.37 (s), 140.34 (s), 140.19 (s), 140.15 (s), 140.08 (s), 137.84 (C-2′′′′′′,6′′′′′′ or C-3′′′′′′,5′′′′′′), 132.07 (d), 131.25 (C-4), 130.81 (d), 130.77 (d), 128.97 (C-2′′′′′′,6′′′′′′ or C-3′′′′′′,5′′′′′′), 128.13 (C-2), 127.80 (d), 127.63 (d), 127.45 (d), 127.34 (d), 127.19 (d), 127.05 (d), 127.01 (d), 123.69 (s), 123.63 (s), 123.60 (s), 122.48 (s), 122.46 (s), 122.41 (s), 122.35 (s), 93.27 (C-4′′′′′′), 90.39 (s), 90.36 (s), 90.25 (s), 89.25 (s), 89.18 (s), 89.11 (s), 83.76 (C-1′′), 77.25 (C-2′′), 35.89 (t), 35.84 (t), 35.79 (t), 31.92 (t), 31.41 (t), 31.37 (t), 31.35 (t), 29.70 (t), 29.68 (t), 29.66 (t), 29.59 (t), 29.58 (t), 29.56 (t), 29.52 (t), 29.50 (t), 29.48 (t), 29.36 (t), 29.34 (t), 29.31 (t), 29.29 (t), 22.68 (t), 14.11 (q); HR-MALDI-MS (dithranol + CF_3CO_2Ag) m/z calcd for $C_{180}H_{241}I - H^+ + 2Ag^+$ $[M - H + 2Ag]^+$ 2742.5921, found 2742.5930.

Cyclic Biphenylene−Acetylene Compound 1. To a degassed solution of CuI (48.6 mg, 0.255 mmol), $Pd(PPh_3)_4$ (94.2 mg, 81.5 μmol), and *N*,*N*-diisopropylethylamine (75 mL) in toluene (275 mL) was added dropwise at 135 °C for 12 h a solution of **26** (104 mg, 41.0 μmol) and *N*,*N*-diisopropylethylamine (25 mL) in toluene (25 mL) divided into six portions. The resulting mixture was stirred at the same temperature for 12 h under an Ar atmosphere. The reaction mixture was poured into a 5% NH_4Cl solution and extracted with dichloromethane. The organic layer was washed with a 5% NH_4Cl solution, dried over $MgSO_4$, and concentrated under reduced pressure. The residue was purified by column chromatography on silica gel with dichloromethane/hexane (1:4) and GPC with chloroform to afford **1** (67.6 mg, 68%). Colorless crystals; mp 163.3−165.1 °C (hexane); IR (KBr disk): $\tilde{\nu}$ = 3037 (w), 2923 (s), 2852 (s), 1590 (m), 1555 (w), 1513 (m), 1490 (w), 1465 (m), 1394 (w), 1369 (w), 1299 (w), 1250 (w), 1183 (w), 1109 (w), 1018 (w), 963 (w), 879 (m), 833 (s), 722 (w), 696 (m), 648 (w), 606 (w), 549 (w), 531 (w) cm^{-1}; UV/vis (CH_2Cl_2): λ (log ε) = 229 (4.93), 235 sh (4.82), 312 (5.41), 328 sh (5.33) nm; ^{1}H NMR (500 MHz, $CDCl_3$, rt): δ = 7.68 (br. s, 6H, 2-H), 7.65 (br. s, 24H, 2′,6′-H and 3′,5′-H), 7.42 (br. s, 6H, 6-H), 7.38 (br. s, 6H, 4-H), 2.69 (br. t, J = 7.5 Hz, 12H, 1′′′-H), 1.69 (br. tt, J = 7.5, 7.1 Hz, 12H, 2′′′-H), 1.43−1.26 (m, 156H, 3′′′-15′′′-H), 0.88 (t, J = 6.9 Hz, 18H, 16′′′-H); ^{13}C NMR (125 MHz, $CDCl_3$, rt): δ = 143.82 (C-5), 140.34 (C-1), 140.16 (C-1′), 132.10 (C-2′,6′ or C-3′,5′), 130.45 (C-4), 128.03 (C-2), 127.11 (C-6), 126.97 (C-2′,6′ or C-3′,5′), 123.65 (C-3), 122.43 (C-4′), 90.36 (C-1″), 89.18 (C-2″), 35.93 (C-1′′′), 31.93 (C-14′′′), 31.43 (C-2′′′), 29.70 (t, 4C), 29.69 (t, 2C), 29.66 (t), 29.60 (t), 29.52 (t), 29.36 (t), 29.34 (t), 22.69 (C-15′′′), 14.12 (C-16′′′); HR-MALDI-MS (dithranol + CF_3CO_2Ag) m/z calcd for $C_{180}H_{240}$ + Ag^+ $[M + Ag]^+$ 2508.7826, found 2508.7854; Anal. Calcd for $C_{180}H_{240}\cdot 1/2H_2O$: C, 89.60; H, 10.07. Found: C, 89.39; H, 9.84.

3-Ethynyl-4′-iodo-5-hexadecylbiphenyl (27). A solution of TBAF (1.0 mol/L, 0.64 mL, 0.64 mmol) in THF was added to a solution of **19** (220 mg, 0.321 mmol) in THF (10 mL). After stirring the mixture at room temperature for 1 h, the reaction mixture was poured into water and extracted with dichloromethane. The organic layer was washed with water, dried over $MgSO_4$, and concentrated under reduced pressure. The residue was purified by column chromatography on silica gel with dichloromethane/hexane (1:4) and GPC with chloroform to afford **27** (154 mg, 91%). Colorless crystals; mp 59.0−59.7 °C (EtOH); IR (KBr disk): $\tilde{\nu}$ = 3313 (m, C≡C−H), 2951 (m), 2919 (s), 2850 (s), 2109 (w, C≡C), 1592 (m), 1562 (w), 1494 (m), 1471 (s), 1444 (w), 1380 (m), 1275 (w), 1180 (w), 1105 (w), 1070 (w), 1004 (m), 895 (w), 877 (m), 850 (w), 820 (s), 717 (m), 697 (m), 639 (w), 612 (w), 588 (m), 493 (w), 466 (w) cm^{-1}; UV/vis (CH_2Cl_2): λ (log ε) = 225 (4.31), 244 sh (4.49), 250 (4.51), 265 (4.35) nm; ^{1}H NMR (500 MHz, $CDCl_3$, rt): δ = 7.75 (d, J = 8.5 Hz, 2H, 2′,6′-H or 3′,5′-H), 7.49 (dd, J = 1.6, 1.3 Hz, 1H, 2-H), 7.33 (br. dd, 1H, 4-H), 7.31 (br. s, 1H, 6-H), 7.30 (d, J = 8.5 Hz, 2H, 2′,6′-H or 3′,5′-H), 3.08 (s, 1H, 2″-H), 2.63 (t, J = 7.8 Hz, 2H, 1′′′-H), 1.63 (tt, J = 7.8, 7.2 Hz, 2H, 2′′′-H), 1.34−1.25 (m, 26H, 3′′′-15′′′-H), 0.88 (t, J = 6.9 Hz, 3H, 16′′′-H); ^{13}C NMR (125 MHz, $CDCl_3$, rt): δ = 143.85 (C-5), 140.19 (C-1 or C-1′), 139.92 (C-1 or C-1′), 137.86 (C-2′,6′ or C-3′,5′), 131.31 (C-4), 128.94 (C-2′,6′ or C-3′,5′), 127.96 (C-2), 127.69 (C-6), 122.50 (C-3), 93.34 (C-4′), 83.65 (C-1″), 77.04 (C-2″), 35.74 (C-1′′′), 31.91 (C-14′′′), 31.31 (C-2′′′), 29.69 (t, 3C), 29.67 (t), 29.65 (t, 2C), 29.64 (t), 29.54 (t), 29.45 (t), 29.35 (t), 29.25 (t), 22.68 (C-15′′′), 14.12 (C-16′′′); HR-MALDI-MS (dithranol + CF_3CO_2Ag) m/z calcd for $C_{30}H_{41}I - H^+ + 2Ag^+$ $[M - H + 2Ag]^+$ 741.0271, found 741.0255; Anal. Calcd for $C_{30}H_{41}I$: C, 68.17; H, 7.82. Found: C, 68.45; H, 7.54.

Cyclic Polyphenylene Array 2. Cyclic biphenylene−acetylene compound **1** (16.1 mg, 6.70 μmol) and **3** (159 mg, 0.414 mmol) was mixed after dissolving into the appropriate amount of THF. After the addition of diphenylether (200 μL) and THF (100 μL) in the well-combined mixture, the combined mixture was stirred at 200−220 °C for 15 h under an Ar atmosphere. The reaction mixture was purified by column chromatography on silica gel with dichloromethane/hexane (1:1) and GPC with chloroform to afford **2** (26.2 mg, 86%) including a small amount of penta-addition product. The isolation of **2** was accomplished by subsequent column chromatography on silica gel

DOI: 10.1021/acs.joc.5b00485
J. Org. Chem. 2015, 80, 5092−5110

with dichloromethane/hexane (2:3). Pale yellow crystals; mp 147.5−149.7 °C (acetone); IR (KBr disk): $\tilde{\nu}$ = 3070 (m), 3050 (m), 3026 (m), 2923 (s), 2853 (s), 1599 (s), 1581 (w), 1514 (w), 1496 (m), 1465 (m), 1442 (s), 1398 (m), 1241 (w), 1176 (w), 1152 (w), 1141 (w), 1107 (w), 1072 (m), 1028 (m), 914 (w), 882 (w), 842 (m), 807 (m), 761 (m), 749 (m), 733 (w), 699 (s), 602 (w), 556 (w) cm^{-1}; UV/vis (CH_2Cl_2): λ (log ε) = 228 (5.49), 254 (5.41), 277 sh (5.35), 307 sh (4.91) nm; ^1H NMR (500 MHz, $CDCl_3$, rt): δ = 6.88−6.42 (br. m, 162H), 2.15 and 2.07 (br. s, 12H), 1.33−1.03 (br. m, 168H), 0.88 (br. t, J = 6.5 Hz, 18H); ^{13}C NMR (125 MHz, $CDCl_3$, rt): δ = 141.19−139.84 (br. s), 131.43 (br., *m*-Ph), 126.50 (br., *o*-Ph), 125.09 (br., *p*-Ph), 36.04−35.53 (br., C-1), 31.99−31.94 (br., C-14), 31.58−31.36 (br., C-2), 30.02−28.96 (br. t), 22.73−22.70 (br., C-15), 14.13 (C-16); HR-MALDI-MS (dithranol + CF_3CO_2Ag) m/z calcd for $C_{348}H_{360}$ + Ag^+ $[M + Ag]^+$ 4645.7216, found 4645.7178; Anal. Calcd for $C_{348}H_{360}$: C, 92.01; H, 7.99. Found: C, 92.03; H, 7.77.

Cyclodehydrogenation Reaction of Polyphenylene Array 2. To a solution of cyclic polyphenylene array **2** (11.7 mg, 2.57 μmol) in dry dichloromethane (45 mL) was added dropwise a solution of anhydrous $FeCl_3$ (276 mg, 1.70 mmol) in nitromethane (2 mL) with argon bubbling. The resulting mixture was stirred at room temperature for 3 days. The reaction was quenched by the addition of methanol (20 mL) in the reaction mixture. The precipitated crystals were corrected by filtration and washed thoroughly with methanol, diluted hydrochloric acid, and water to afford dark brown solid (8.9 mg) that is hardly soluble in common organic solvents. The solid was used directly for MALDI-TOF MS measurement without further purification.

■ ASSOCIATED CONTENT

Supporting Information

General experimental details. Physical data (solid-state FL experiments, FL decay profiles, DSC thermograms, X-ray diffraction powder patterns) of **1** and **2**. NMR spectra of novel compounds. Results of the theoretical calculations with optimized Cartesian coordinates. The Supporting Information is available free of charge on the ACS Publications website at DOI: 10.1021/acs.joc.5b00485.

■ AUTHOR INFORMATION

Corresponding Author

*E-mail: itsnj@hirosaki-u.ac.jp.

Notes

The authors declare no competing financial interest.

■ ACKNOWLEDGMENTS

The present work was supported by JSPS KAKENHI Grant Number 24550037 to S.I.

■ REFERENCES

(1) Recent review of CCPs: (a) Jasti, R.; Bertozzi, C. R. *Chem. Phys. Lett.* **2010**, *494*, 1−7. (b) Hirst, E. S.; Jasti, R. *J. Org. Chem.* **2012**, *77*, 10473−10478. (c) Omachi, H.; Segawa, Y.; Itami, K. *Acc. Chem. Res.* **2012**, *45*, 1378−1389. (d) Yamago, S.; Kayama, E.; Iwamoto, T. *Chem. Rec.* **2014**, *14*, 84−100. (e) Bunz, U. H. F.; Menning, S.; Martín, N. *Angew. Chem., Int. Ed.* **2012**, *51*, 7094−7101.

(2) (a) Jasti, R.; Bhattacharjee, J.; Neaton, J. B.; Bertozzi, C. R. *J. Am. Chem. Soc.* **2008**, *130*, 17646−17647. (b) Sisto, T. J.; Golder, M. R.; Hirst, E. S.; Jasti, R. *J. Am. Chem. Soc.* **2011**, *133*, 15800−15802. (c) Xia, J.; Jasti, R. *Angew. Chem., Int. Ed.* **2012**, *51*, 2474−2476. (d) Darzi, E. R.; Sisto, T. M.; Jasti, R. *J. Org. Chem.* **2012**, *77*, 6624−6628.

(3) (a) Takaba, H.; Omachi, H.; Yamamoto, Y.; Bouffard, J.; Itami, K. *Angew. Chem., Int. Ed.* **2009**, *48*, 6112−6116. (b) Omachi, H.; Matsuura, S.; Segawa, Y.; Itami, K. *Angew. Chem., Int. Ed.* **2010**, *49*, 10202−10205. (c) Segawa, Y.; Šenel, P.; Matsuura, S.; Omachi, H.; Itami, K. *Chem. Lett.* **2011**, *40*, 423−425. (d) Ishii, Y.; Nakanishi, Y.; Omachi, H.; Matsuura, S.; Matsui, K.; Shinohara, H.; Segawa, Y.; Itami, K. *Chem. Sci.* **2012**, *3*, 2340−2345. (e) Sibbel, F.; Matsui, K.; Segawa, Y.; Studer, A.; Itami, K. *Chem. Commun.* **2014**, *50*, 954−956.

(4) (a) Yamago, S.; Watanabe, Y.; Iwamoto, T. *Angew. Chem., Int. Ed.* **2010**, *49*, 757−759. (b) Segawa, Y.; Miyamoto, S.; Omachi, H.; Matsuura, S.; Šenel, P.; Sasamori, T.; Tokitoh, N.; Itami, K. *Angew. Chem., Int. Ed.* **2011**, *50*, 3244−3248. (c) Iwamoto, T.; Watanabe, Y.; Sakamoto, Y.; Suzuki, T.; Yamago, S. *J. Am. Chem. Soc.* **2011**, *133*, 8354−8361. (d) Kayahara, E.; Sakamoto, Y.; Suzuki, T.; Yamago, S. *Org. Lett.* **2012**, *14*, 3284−3287. (e) Kayahara, E.; Iwamoto, T.; Suzuki, T.; Yamago, S. *Chem. Lett.* **2013**, *42*, 621−623. (f) Kayahara, E.; Patel, V. K.; Yamago, S. *J. Am. Chem. Soc.* **2014**, *136*, 2284−2287.

(5) Omachi, H.; Segawa, Y.; Itami, K. *Org. Lett.* **2011**, *13*, 2480−2483.

(6) Yagi, A.; Segawa, Y.; Itami, K. *J. Am. Chem. Soc.* **2012**, *134*, 2962−2965.

(7) Yagi, A.; Venkataramana, G.; Segawa, Y.; Itami, K. *Chem. Commun.* **2014**, *50*, 957−959.

(8) Matsuno, T.; Kamata, S.; Hitosugi, S.; Isobe, H. *Chem. Sci.* **2013**, *4*, 3179−3183.

(9) Hitosugi, S.; Nakanishi, W.; Yamasaki, T.; Isobe, H. *Nat. Commun.* **2011**, *2*, 492.

(10) Hitosugi, S.; Yamasaki, T.; Isobe, H. *J. Am. Chem. Soc.* **2012**, *134*, 12442−12445.

(11) (a) Sisto, T. J.; Tian, X.; Jasti, R. *J. Org. Chem.* **2012**, *77*, 5857−5860. (b) Nishiuchi, T.; Feng, X.; Enkelmann, V.; Wagner, M.; Müllen, K. *Chem.—Eur. J.* **2012**, *18*, 16621−16625. (c) Golling, F. E.; Quernheim, M.; Wagner, M.; Nishiuchi, T.; Müllen, K. *Angew. Chem., Int. Ed.* **2014**, *53*, 1525−1528.

(12) Xia, J.; Golder, M. R.; Foster, M. E.; Wong, B. M.; Jasti, R. *J. Am. Chem. Soc.* **2012**, *134*, 19709−19715.

(13) (a) Gleiter, R.; Esser, B.; Kornmayer, S. C. *Acc. Chem. Res.* **2009**, *42*, 1108−1116. (b) Steinberg, B. D.; Scott, L. T. *Angew. Chem., Int. Ed.* **2009**, *48*, 5400−5402.

(14) (a) Nakamura, E.; Tahara, K.; Matsuo, Y.; Sawamura, M. *J. Am. Chem. Soc.* **2003**, *125*, 2834−2835. (b) Matsuo, Y.; Tahara, K.; Morita, K.; Matsuo, K.; Nakamura, E. *Angew. Chem., Int. Ed.* **2007**, *46*, 2844−2847.

(15) Korich, A. L.; McBee, I. A.; Bennion, J. C.; Gifford, J. I.; Hughes, T. S. *J. Org. Chem.* **2014**, *79*, 1594−1610.

(16) Komatsu, N. *Jpn. J. Appl. Phys.* **2010**, *49*, 02BC01.

(17) Ito, S.; Wehmeier, M.; Brand, J. D.; Kübel, C.; Epsch, R.; Rabe, J. P.; Müllen, K. *Chem.—Eur. J.* **2000**, *6*, 4327−4342.

(18) Miller, T. M.; Neenan, T. X.; Zayas, R.; Bair, H. E. *J. Am. Chem. Soc.* **1992**, *114*, 1018−1025.

(19) Félix, G.; Dunoguès, J.; Pisciotti, F.; Calas, R. *Angew. Chem., Int. Ed. Engl.* **1977**, *16*, 488−489.

(20) Theoretical calculations were performed using *Spartan '10*, Wavefunction, Inc.: Irvine, CA, 2011.

(21) (a) Mindyuk, O. Y.; Stetzer, M. R.; Heiney, P. A.; Neelson, J. C.; Moore, J. S. *Adv. Mater.* **1998**, *10*, 1363−1366. (b) Zhang, J.; Moore, J. S. *J. Am. Chem. Soc.* **1994**, *116*, 2655−2656.

(22) (a) Tauchi, L.; Nakagaki, T.; Shimizu, M.; Itoh, E.; Yasutake, M.; Ohta, K. *J. Porphyrins Phthalocyanines* **2013**, *17*, 1080−1093. (b) Ishikawa, A.; Ono, K.; Ohta, K.; Yasutake, M.; Ichikawa, M.; Itoh, E. *J. Porphyrins Phthalocyanines* **2014**, *18*, 366−379.

(23) Yoshimura, K.; Przybilla, L.; Ito, S.; Brand, J. D.; Wehmeier, M.; Räder, H. J.; Müllen, K. *Macromol. Chem. Phys.* **2001**, *202*, 215−222.

DOI: 10.1021/acs.joc.5b00485
J. Org. Chem. 2015, 80, 5092−5110